

N70-28148

TM-70-1014-2

# TECHNICAL MEMORANDUM

## MULTIPLE SCATTERING CALCULATION FOR PLANETARY ATMOSPHERES

CASE FILE  
COPY

Bellcomm

**NASA FILE COPY**

Library in  
NASA HQ. LIBRARY (USS-10)  
WASHINGTON, D.C. 20546-STEP-01  
STEP-01

**HQ. LIBRARY (USS-10)**

BELLCOMM, INC.

955 L'ENFANT PLAZA NORTH, S.W. WASHINGTON, D.C. 20024

COVER SHEET FOR TECHNICAL MEMORANDUM

TITLE- Multiple Scattering Calculation  
for Planetary Atmospheres

TM- 70-1014-2

DATE- May 15, 1970

FILING CASE NO(S)- 235

AUTHOR(S)- E. N. Shipley

FILING SUBJECT(S)- Planetary Atmosphere  
(ASSIGNED BY AUTHOR(S)- Multiple Scattering  
Martian Haze

ABSTRACT

An iterative technique for calculating the multiple scattering effect in planetary atmospheres has been developed. Various studies have been conducted to insure the accuracy of the technique and of the computer programs which carry out the calculations.

The technique, while intended for a spherical geometry, can be adapted to a planar geometry, for which exact calculations are available through the method developed by Chandrasekhar. Comparisons of the apparent brightness were made for a haze model which had been developed previously to explain the photometric results of Mariner IV. For the planar geometry, the iterative technique produces results which agree with the exact calculations to better than 1/2%.

For the spherical geometry, it was found that the effect of multiple scattering was to increase the apparent brightness by about 20% when the line of sight intersected the surface, and by up to a factor of two when the line of sight lies above the limb of the planet.

It is concluded that the iterative technique provides an accurate method of calculating multiple scattering effects in planetary atmospheres.

BA-145A (8-68)

SEE REVERSE SIDE FOR DISTRIBUTION LIST

DISTRIBUTION

COMPLETE MEMORANDUM TO

CORRESPONDENCE FILES:

OFFICIAL FILE COPY

plus one white copy for each  
additional case referenced

TECHNICAL LIBRARY (4)

NASA Headquarters

- W. O. Armstrong/MTX
- P. E. Culbertson/MT
- N. W. Cunningham/SL
- E. W. Glahn/SL
- E. W. Hall/MTG
- H. F. Hipsher/SL
- W. Jakobowski/SL
- T. A. Keegan/MA-2
- R. Kraemer/SL
- R. L. Lohman/MF
- D. R. Lord/MF
- M. Mitz/SL
- L. Roberts/MTG (2)
- A. D. Schnyer/MTE
- M. G. Waugh/MT-1
- J. W. Wild/MTE

NASA Headquarters Library  
(USS-10) (2)

Goddard Space Flight Center

- R. A. Hanel/620
- C. C. Stephanides/620

Jet Propulsion Laboratory

- R. A. Becker/323
- S. Z. Gunter/329
- A. J. Kliore/311
- J. Lorell/311
- J. A. Stallkamp/241
- R. H. Steinbacher/32
- A. T. Young/323

Langley Research Center

- G. A. Soffen/159
- I. Taback/159
- A. T. Young/159

Manned Spacecraft Center

- C. R. Hicks/FA4

COMPLETE MEMORANDUM TO

California Institute of Technology

- N. H. Horowitz
- R. B. Leighton
- B. C. Murray
- G. Neugebauer
- R. P. Sharp

Cornell University

- J. B. Pollack
- C. Sagan

Massachusetts Institute  
of Technology

- T. B. McCord
- I. I. Shapiro

New Mexico State University

- B. Smith

Rand Corporation

- M. E. Davies

Stanford University  
School of Medicine

- J. Lederberg
- E. Levinthal

University of Arizona

- W. K. Hartman

University of Colorado

- C. A. Barth

University of Texas

- G. de Vaucouleurs

University of Washington

- C. Leovy

USGS-Flagstaff, Arizona

- R. M. Batson
- W. T. Borgeson
- H. Masursky
- R. L. Wildey

DISTRIBUTION LIST (CONT'D.)

COMPLETE MEMORANDUM TO

USGS - Menlo Park, California

M. H. Carr  
J. F. McCauley  
D. J. Milton  
D. E. Wilhelms

Bellcomm, Inc.

G. M. Anderson  
A. P. Boysen, Jr.  
C. L. Davis  
D. A. De Graaf  
D. R. Hagner  
N. W. Hinners  
B. T. Howard  
D. B. James  
J. Kranton  
H. S. London  
K. E. Martersteck  
R. K. McFarland  
J. Z. Menard  
G. T. Orrok  
F. N. Schmidt  
R. V. Sperry  
W. Strack  
W. B. Thompson  
J. E. Waldo  
M. P. Wilson  
All Members Division 101  
Central Files  
Department 1024 File  
Library

Abstract Only to

Bellcomm, Inc.

I. M. Ross  
J. W. Timko  
R. L. Wagner

**BELLCOMM, INC.**

955 L'ENFANT PLAZA NORTH, S.W. WASHINGTON, D. C. 20024

**SUBJECT:** Multiple Scattering  
Calculation for Planetary  
Atmospheres - Case 235

**DATE:** May 15, 1970

**FROM:** E. N. Shipley

TM-70-1014-2

TECHNICAL MEMORANDUM

1.0 INTRODUCTION

The purpose of this memorandum is to report on efforts to carry out multiple scattering calculations for planetary atmospheres. The specific problem for which the calculations have been made is the scattering of light in the Martian haze that has been suggested<sup>(1)</sup> to explain the data from Mariner IV.

The properties of such a Martian haze have already been studied in considerable detail on the basis of first-order calculations.<sup>(2)</sup> However, it was recognized that multiple scattering processes would cause a major effect, and would have to be included in the calculations in order to obtain useful accuracy. A method to carry out the multiple scattering calculations has been developed. In this memorandum, some preliminary calculations which were used to test the validity and accuracy of the method are reported.

The Martian haze was evoked to explain the observations made by Mariner IV. However, similar phenomena were not observed in the recent Mariner VI and VII missions. This has given additional credence to the suspicion that the data from Mariner IV were affected by a malfunction in the camera or spacecraft system,<sup>(1)(3)</sup> although this opinion does not have universal acceptance.

\* Our purpose here is not to argue the reality of the haze, but to verify the accuracy of a procedure to perform multiple scattering calculations. The haze is a convenient model to use because of the previous work with which the calculations can be compared.

In particular, exact multiple scattering calculations have been carried out<sup>(2)</sup> using the classic methods developed by Chandrasekhar.<sup>(4)</sup> The exact calculations of Chandrasekhar are applicable only to planar atmospheres, while it is necessary, in our case, to consider the spherical geometry of the planet. For example, the brightness above the limb of a planet has no parallel in planar atmospheres.

The procedure that has been developed can be adapted to either spherical or planar geometry. The results of the planar case, compared with the exact calculations, give an indication of the overall accuracy of the technique. In addition, results for the spherical geometry have been included to illustrate the effect of multiple scattering in that case.

It is worth noting that the procedures developed for multiple scattering calculations are applicable to problems other than Martian haze. At the present time, the area of greatest interest is Rayleigh scattering in the gaseous atmosphere of Mars. Preliminary calculations(5) have been carried out to illustrate how brightness measurements above the limb of a planet can be used to deduce the density profile of the atmosphere. Multiple scattering effects must be included in the atmospheric problem in order to achieve high accuracy.

In some of the following discussions, the comments do not depend on the particular properties of the material surrounding the planet. In such cases the term "atmosphere" has been used in a general sense to refer to any medium surrounding a planet.

## 2.0 METHOD

The brightness seen by an observer looking through a planetary atmosphere or a haze obeys the relation

$$\frac{d\omega}{d\chi} = -\sigma(\chi)\omega(\chi, 0, 0) + \beta(\chi, \theta_s)\pi F e^{-\tau_s} + \int \beta(\chi, \theta)\omega(\chi, \theta, \phi)d\Omega \quad (1)$$

where  $\omega(\chi, \theta, \phi)$  is the luminous intensity at the point  $\chi$  incident on a volume element from a direction whose polar coordinates are  $\theta, \phi$  (see Figure 1). The direction  $\theta=0$  corresponds to light moving toward the observer.  $\pi F$  is the flux in the incident solar radiation,  $\theta_s$  is the polar angle for the direction of the incident radiation, and  $\tau_s$  is the optical thickness between the source of the incident radiation and the volume element at the point  $\chi$ . The distance  $\chi$  is measured along the line of sight, increasing toward the observer.

$\beta(\chi, \theta)$  is the fraction of the incident light in a unit solid angle that is scattered into a unit solid angle centered at an angle  $\theta$  to the initial direction, per unit length travelled by the light. The function  $\beta$  describes completely the scattering properties of the atmosphere or haze. The function  $\sigma(\chi)$  represents the extinction coefficient for the atmosphere. The dependence on  $\chi$  for both  $\beta(\chi, 0)$  and  $\sigma(\chi)$  arises from variations of the density of the atmosphere.

In the case of isotropic scattering, with which we will be exclusively concerned in this memorandum,  $\beta$  does not depend on  $\theta$ .

We may define the scattering coefficient  $b$  through the relation

$$b(\chi) = \int \beta(\chi, \theta) d\Omega = 4\pi\beta \quad (2)$$

and Equation(1) may be written

$$\frac{d\omega}{d\chi} = -\sigma(\chi) \omega(\chi, 0, 0) + \frac{b(\chi)}{4\pi} \pi F e^{-\tau} s + \frac{b}{4\pi} \int \omega(\chi, \theta, \phi) d\Omega \quad (3)$$

In Equation (1), the first term on the right hand side accounts for the attenuation of the light already travelling toward the observer, the second term corresponds to scattering of the incident solar radiation, and the third term comes from the scattering of the diffuse light incident on the volume element at  $\chi$  from the surrounding haze and the surface of the planet. It is the third term in Equation(1), the integral, that accounts for the multiple scattering, since it represents the scattering of light which has already been scattered at least once. In the first order calculations, where only a single scattering is considered, the integral is neglected. A more detailed discussion of Equation (1) has been given previously(2).

The integro-differential equation (1) can be solved exactly for planar atmospheres with a plane parallel beam of radiation incident on the atmosphere(4). However, for a spherical atmosphere with a plane parallel incident beam, no such solution is known. An accurate approximate solution can be obtained by numerical methods, as follows:(6)

Suppose we have an estimate of the brightness at each point in the atmosphere, for all directions. We call such an estimate a data base. The data base consists of a list of brightness values for certain directions at a selected set of points throughout the atmosphere. The geometry is shown in Figure 2. A point in the atmosphere is defined by  $\lambda$ , the sun angle, and  $h$ , the height above the surface. Cylindrical symmetry is assumed to exist about the direction of solar radiation. The angles  $\theta$  and  $\phi$  define a local polar coordinate system in which the direction of the incident radiation is measured.

The atmospheric brightness data is stored for a finite set of points distributed throughout the atmosphere. These local points are defined by the intersection of lines of constant height,  $h_j$  and lines of constant sun angle,  $\lambda_i$ , where the values  $h_j, \lambda_i$  are chosen to meet the requirements of the problem. At each local point, the brightness is stored for each of a set of directions defined by the angles  $\theta_k, \phi_k$ . This set of angles is the same for each local point.

At each local point, there is reflection symmetry in the plane defined by the direction of the incident radiation and the radius vector from the center of the planet. This symmetry is a direct result of the overall cylindrical symmetry of the problem. Thus the set of angles  $\theta_k, \phi_k$  may be chosen to cover only a hemisphere, or more specifically

$$0 \leq \phi_k \leq \pi$$

The brightness value for an arbitrary point in the atmosphere and for an arbitrary direction can be obtained through interpolation among values in the data base. In this way, the value of the integral in Equation (1) may be evaluated for any point in the atmosphere, and the equation can be solved by standard numerical techniques. It is clear that the accuracy of the numerical techniques will depend on the selection of matrix points for the data base, and that increasing the density of points will lead to improved accuracy.

The data base itself is constructed by an iterative procedure. In the zeroth order data base, all of the brightness values for the atmosphere are set equal to zero. This is equivalent to setting the integral in Equation (1) to zero. The next higher order data base is obtained by solving Equation (1) for the complete set of direction angles for all local points; the solutions are obtained using the zeroth order data base to evaluate the integral in Equation (1). Successive iterations lead to a data base of sufficient accuracy for the required solution.

All of the computational work is done on a Univac 1108 computer. A group of programs has been written to manipulate the data base. There are programs to move the data base between tape storage and random access bulk storage, set up the zeroth order data base, perform an iteration on the data base, compute the change in the data produced by an iteration, or solve Equation (1) in a specified geometry using the best available data base.

### 3.0 PLANAR ATMOSPHERE

The light scattered by a planar haze can be calculated exactly by a method developed by Chandrasekhar. These calculations, which we will refer to as the "exact calculations", can serve as a convenient reference against which to compare the results of the iterative procedure developed for use in the spherical case.



For the iterative calculations, the change from the spherical to the planar case requires only a few minor changes in the geometrical calculations involved in the program. The main features of the program are identical in the two cases. Because of this, agreement between the iterative and the exact calculations serves to indicate not only the validity and accuracy of the approach, but also the correctness of the computer program written to carry out the calculations. This is extremely important because in computer programs as long and as complicated as those involved here it is very easy for programming errors to go undetected.

The haze model that is the basis of the computations is the same as that described previously<sup>(2)</sup>. Throughout this report, a cutoff altitude of 122.3035 km has been used. (The cutoff altitude is the altitude below which no haze exists). The value used differs slightly from previous values in order that the optical thickness of the haze be almost 0.4, an essential feature to simplify the exact calculations<sup>(2)</sup>. Table I lists the parameters which describe the haze.

A major question for the iterative calculations is the rapidity with which they converge to a solution of acceptable accuracy. The convergence properties are shown in Figure 3 for a sun angle of  $0^\circ$  and in Figure 4 for a sun angle of  $60^\circ$ . It should be noted that, because of the symmetry inherent in isotropic scattering in a planar atmosphere, there is no dependence on the azimuthal angle between the sun direction and the viewing direction.

All the brightness values shown in the curves for this report are given relative to the brightness of an ideal Lambert surface normal to the incident solar radiation (and without any haze). For convenience, we use the term millilamb to indicate one one-thousandth of the brightness of such a reference surface.

In both Figure 3 and Figure 4, it is apparent that after just four iterations, the iterative solution closely approximates the exact values. Further iterations, which are not illustrated in the figures, bring the iterative and exact calculations into agreement of better than 1/2%. It should be noted that the accuracy of the exact calculations is itself limited to 1/2%; this uncertainty arises from the evaluation of the functions described by Chandrasekhar and in the numerical integrations required to obtain the actual numbers.

For the remainder of this section, the data base used for the calculations was created through 12 iterations. During the last iteration, the maximum change that occurred for any point in the data base was 0.1%.

In Figures 3 and 4, the effect of the multiple scattering is to increase the brightness about 30% above the first estimate (NIT = 0). Because the multiple scattering represents such a small portion of the final result, the agreement shown in these figures is not a sensitive indicator of the accuracy of the iterative technique.

A more sensitive indicator is a measurement of the multiply scattered light itself. The first two terms in Equation (1) present no computational problem since they can be calculated with high accuracy for any point in the atmosphere. The difficulty is to obtain the brightness values for the integrand of the third term in the equation, which, as we noted before, gives rise to multiple scattering. The integrand is just the diffuse light in the atmosphere (the term diffuse is used to provide a distinction between it and the plane parallel solar radiation). In the zeroth approximation the diffuse light is zero. The accuracy with which it is calculated in the final approximation serves as a sensitive indication of the overall accuracy of the multiple scattering procedure.

The diffuse light incident on the surface is shown in Figures 5 and 6, for sun angles of  $0^\circ$  and  $30^\circ$ , respectively, for both the iterative and the exact calculations. It is readily apparent from these graphs that there is extremely good agreement between the two calculations. This is a significant indication that the iterative technique converges correctly to the desired solution.

Similarly, Figure 7 shows the surface illumination as a function of sun angle. This curve indicates good agreement is achieved by the iterative calculations for the full range of sun angles.

Thus it may be concluded that the iterative technique provides accurate results for a planar atmosphere. The accuracy is at least as good as 1/2%. Part of this observed discrepancy may arise in the numerical integrations used to obtain the exact results.

The success of the iterative technique indicates, in addition, that the computer program is error free, to a high degree of certainty.

#### 4.0 SPHERICAL GEOMETRY

The most obvious difference between the spherical and planar calculations is in the geometrical calculations. While the differences are significant, they represent straightforward calculations and cause no conceptual or programming difficulty.

A more subtle difference between the spherical and planar cases arises because of various discontinuities in brightness which are a part of the spherical problem. Discontinuities are the bane of numerical integrations. Either care must be exercised to account for the discontinuities in the integration procedure, or they will represent a source of error in the computations.

In developing the iterative technique, care was exercised to take into account discontinuities where they could have a significant impact on the results. Figure 8 shows the discontinuities along a typical line of sight through the atmosphere. Discontinuities arise where the line of sight enters or leaves the limited region where the haze exists, and where the line of sight enters or leaves the shadow zone. Entering or leaving the haze region gives rise to a discontinuity in the density of the haze, and hence in the extinction and scattering coefficients in Equation (3). The boundary of the shadow zone represents a discontinuous change in the incident solar radiation.

Integration of Equation (1) along the line of sight is accomplished by the rectangle method; the value of the derivative is calculated at a point and multiplied by the length of a short interval surrounding the point. The points were chosen so that all discontinuities lie on the border of two adjacent intervals.

Another discontinuity, which was not illustrated in Figure 8, occurs when the line of sight intersects the surface of the planet. This discontinuity, and some of those corresponding to entering and leaving the region of haze, represent just the initial and final points of the range of integration. All of the discontinuities occurring along the line of sight have been accounted for exactly, and hence do not affect the accuracy of the calculations in the spherical geometry.

However, discontinuities may affect the evaluation of the integral in Equation (1). This integral represents the integration of light incident at the reference point from all directions. There is a discontinuity in the incident radiation corresponding to the horizon; in most circumstances the surface area below the horizon is markedly brighter than the atmosphere above the horizon.

The integral is evaluated by summing the products of the brightness in specific directions (the selected directions in the data base) and the solid angle contained in an area surrounding the direction. The discontinuity will cause an error if the horizon does not occur on the border of these areas. If a border does correspond to the horizon, an accurate evaluation will result since brightness representative of the surface (or the atmosphere) will be used for a solid angle corresponding to that actually subtended by the surface (or atmosphere).

The angle between the horizon and the local vertical depends on the altitude above the surface. It is  $90^\circ$  at the surface,  $105^\circ$  at the low altitude cutoff (122.3 km) and  $109^\circ$  at the high altitude limit of the atmosphere.

The directions for which brightness values are stored in the data base are given in Table II. Data is stored for polar angles of  $90^\circ$  and  $120^\circ$ , so that the border between them lies at  $105^\circ$ , close to the horizon. In the worst case, when the horizon is at  $109^\circ$  below local vertical, 3.6% of the solid angle would be misplaced, that is, calculated as if it has surface brightness when in fact it corresponds to atmosphere. Moreover, the greatest error occurs where the haze is thinnest; consequently the error has a minimal effect on the observed brightness.

Although the horizon problem is not critical for the haze calculations, provided the polar directions for the data base are carefully chosen, the problem will be significant in cases where the scattering medium extends down to the surface. Specifically, for calculations of the brightness of the gaseous atmosphere of Mars, additional consideration must be given to this problem.

Discontinuities can also cause computational errors in another context. At regular intervals along the line of sight, points are selected for the evaluation of Equation (1). In general, these points do not correspond to points contained in the data base. In order to evaluate the integral in Equation (1), a linear interpolation is performed among the nearest points in the data base. In certain circumstances, adjacent data base points have different geometrical properties (such as shadowing). The interpolation procedure does not take into account the geometry of the data base points relative to the point at which the evaluation is being made, and where there are such differences among the data base points the interpolation does not give an accurate value. This does not cause a serious error to the overall calculation

because it occurs in a limited geometrical region and because the values are small in the regions, near the terminator, where it does occur.

Interpolation problems can also arise in areas where the brightness changes rapidly. Such a region is the lower part of the haze, where the absolute value of the density changes most quickly. If the local points were spaced equally in height, major changes in brightness would occur between adjacent height points, and an inaccurate interpolation would result. Instead, the height points were chosen to maintain an equal vertical optical thickness between points. However, the rule was not used for the upper portion of the atmosphere, where it would make the distance between points excessive. In the upper regions, uniform height spacing was used. This is shown in Table III, which gives the matrix of the local points.

Problems similar to those described above do not occur for the planar case. There are no shadows in the planar case. The discontinuities at the top and bottom of the haze are treated in the same way as for the spherical case, and so are accounted for exactly. The horizon is at  $90^\circ$  regardless of the height above the surface, and the polar angles for the planar case were chosen so that there was a border at  $90^\circ$ . Neither does the interpolation procedure cause a problem in the planar case because, for a given calculation, all points have the same sun angle and essentially the same geometry.

Convergence properties for the spherical geometry are shown in Figure 9 for a sun angle of  $0^\circ$ . It is clear that the convergence is extremely rapid. The observed change between  $NIT = 4$  and  $NIT = 10$  was less than 0.1% for  $0^\circ$  sun angle.

However, certain points in the data base continue to change even for  $NIT = 7$ . This is shown in Figure 10, which shows in histogram form the number of points in the data base which have undergone changes of various amounts. For  $NIT = 7$ , a small portion of the points in the data base show a modest increase up to about 1/2%. These points in general have low absolute value and lie primarily in regions near the terminator. Hence they do not affect significantly those points having a sun angle of  $0^\circ$ .

Figure 10 also shows a histogram for  $NIT = 10$ . At this point, no significant changes occur for any point in the data base.

Typical results of the multiple scattering calculations are shown in Figures 11 through 14. The first three of these figures allow a comparison to be made among the various types of calculations: multiple scattering for a spherical geometry, multiple scattering for a planar geometry, and first order calculations (NIT = 0) for a spherical geometry. Comparison of the first order and multiple scattering results for the spherical case indicate that the multiple scattering produces an increase of about 20% in the apparent brightness. Note, however, that the line of sight in these figures intersects the surface, and a major portion of the apparent brightness arises from light scattered from the surface. This is shown in Figure 11, where the lowest curve gives the apparent brightness that would be observed if the light scattered by the haze is not included; attenuation by the haze has been included. From a comparison of the increased brightness due to first order calculations with that due to multiple scattering, it is apparent that multiple scattering approximately doubles the effect of the haze in increasing the brightness.

The surface contribution is also shown in Figure 13 for a sun angle of  $60^\circ$ . The effect of multiple scattering, compared to the first order calculation, is not as great as for a sun angle of  $0^\circ$ ; nevertheless it still represents a substantial contribution to the apparent brightness.

In the spherical geometry, the apparent brightness depends on the azimuthal angle between the direction of the incident solar radiation and the viewing direction (the geometry is shown in Figure 2). The range of values of the apparent brightness as the azimuthal angle is varied from  $0^\circ$  to  $180^\circ$  is indicated by cross hatching in Figures 12 through 14. For a sun angle of  $0^\circ$  (Figure 11), symmetry precludes any azimuthal dependence.

For sun angle of  $80^\circ$  or less, and for any look angle, the brightness decreases monotonically as the phase angle goes from  $0^\circ$  to  $180^\circ$ . Thus the upper boundary line of the cross-hatched area represents  $0^\circ$  azimuthal angle, and the lower boundary line an azimuth of  $180^\circ$ .

This relationship does not hold at a sun angle of  $90^\circ$ . In Figure 15, the apparent brightness for different azimuthal angles are shown for a sun angle of  $90^\circ$ . It is quite apparent that for look angles near  $90^\circ$  and for azimuthal angles near  $180^\circ$ , there is considerable structure in the brightness profiles. The structure arises from the interaction of the shadow zone and the haze-free region below the cutoff. That is to say that the structure depends on the detailed geometry of the haze, and even slight changes in the haze model would cause significant variation in the structure.

Conversely, detailed observations of the brightness in the region near the terminator (sun angle =  $90^\circ$ ) can be used to infer the structure of the haze. This point has been discussed previously<sup>(2)</sup>.

There are no exact calculations against which the results of the spherical geometry may be compared. A crude estimate of the validity may be obtained by a comparison with the results from the planar geometry, however. The relationship between the geometry from the spherical and planar cases is shown in Figure 16. When both the look angle and the sun angle are near  $0^\circ$ , the planar geometry is an approximation to that of the spherical case. As either the sun or the look angle changes from  $0^\circ$ , the quality of the approximation is degraded.

A comparison of the calculations for the flat and the spherical geometry in Figures 11 through 14 indicates that the behavior of the apparent brightness is consistent with the quality of the approximation. It is not possible to make the comparison quantitative since there are systematic differences between the flat and spherical cases even for  $0^\circ$ .

It is also of major importance to study the brightness above the limb of the planet. The geometry for this viewing is shown in Figure 17. The brightness profile above the limb is itself shown for two different sun orientations in Figures 18 and 19; Figure 20 displays the specific orientations used.

Figure 18 gives the brightness profile for the Mariner IV geometry; that is, the profile corresponds to the region above the limb which was photographed in the first Mariner IV picture. The first order calculations are shown for comparison. It should be noted that the brightness above the limb is essentially constant up to an altitude of about 150 km. Beyond that, the brightness falls off rapidly. This constancy of brightness occurs despite the structure of the haze. It is necessary for the brightness profile to have this characteristic in order to account for the Mariner IV data.

Figure 19 displays the brightness profile for the case where the line of sight passes above the sub-solar point. It is clear from Figure 19 that the multiple scattering effect can change the apparent brightness by a factor of two above the first order calculation. The actual effect, of course, depends on the precise geometry, and the effect is smaller when the sun angle ( $\sigma$ ) nears  $90^\circ$ . The important point, however, is that multiple scattering does change the brightness above the limb by a substantial amount.

## 5.0 CONCLUSIONS

The accuracy of the iterative technique for performing multiple scattering calculations has been illustrated for a planar atmosphere by showing that the calculations agree with exact results computed by the method of Chandrasekhar. Furthermore, it has been shown that the iterative calculations for the spherical geometry behave as expected. Hence it is concluded that the iterative technique provides an accurate method of performing multiple scattering calculations for planetary atmospheres. A subsidiary conclusion is that the computer programs developed to carry out the calculations are likewise accurate.

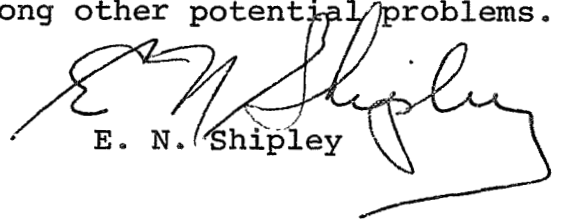
Results were presented for the apparent brightness for Mars under certain geometric conditions with the assumption that a specific haze model described the optical properties above the surface of the planet. The haze model was developed through the use of first order calculations, and the parameters of the model were chosen to give good agreement between the first order calculations and the Mariner IV data<sup>(2)</sup>. Because multiple scattering causes substantial changes in the brightness compared to first order estimates, the multiple scattering results are not suitable for comparison with Mariner IV data. It will be necessary to adjust the parameters of the haze model to bring the new results into agreement with the observed data.

Because the multiple scattering affects the apparent brightness above the limb to a much greater degree than the apparent brightness of the surface, it is believed that a major variation of the parameters, at least, will be required, and it may be necessary to alter significantly the structure of the haze.

The computational technique itself can be improved to eliminate the remaining problems with the discontinuities that were described earlier. A new technique for handling the horizon discontinuity in the integral of Equation (1) is necessary in order to permit the calculations to be used for atmospheres which extend down to the surface (a suitable method has already been developed), and a better interpolation procedure is desirable in order to increase confidence in the accuracy of the spherical calculations.



However, the important point is that a technique now exists to carry out multiple scattering calculations in a spherical geometry with incident solar radiation. The technique can be applied both to the possible Martian haze and to scattering in the gaseous atmosphere of Mars, among other potential problems.



E. N. Shipley

1014-ENS-bmn

Attachments  
References  
Tables I-III  
Figures 1-20

# BELLCOMM, INC.

## REFERENCES

1. P. L. Chandeysson, E. N. Shipley and W. B. Thompson, "Haze in the Mars Atmosphere as Revealed by the Mariner IV Television Data," Bellcomm, Inc. TR-68-710-6, August 20, 1968.
2. E. N. Shipley, "A Model of the Martian Haze," Bellcomm, Inc. TR-69-235-1, July 14, 1969.
3. A. T. Young, Icarus 11, 1 (1969).
4. S. Chandrasekhar, Radiative Transfer, Dover Publications, New York (1960).
5. E. N. Shipley, "Preliminary Investigations of the Use of Photographic Measurements of the Atmospheric Brightness of Mars to Study the Atmospheric Structure," Bellcomm, Inc., June 19, 1969.
6. Reference 2, Appendix A.

TABLE I  
PARAMETERS OF THE HAZE MODEL

Scale height, $h_0$	10 km
Low altitude cutoff, $h_{CO}$	122.3 km
High altitude cutoff, $h_{max}$	200 km
Surface normal albedo, $\rho$	0.5
Albedo for single particle scattering, $\rho_s$	0.5
Extinction coefficient extrapolated to the surface, $\sigma_0$	8200 km <sup>-1</sup>

Scattering coefficient  $b = \rho_s \sigma$ , where

Extinction coefficient $\sigma = \sigma_0 e^{-h/h_0}$	$h_{CO} < h < h_{max}$
$\sigma = 0$	$h < h_{CO}$
$\sigma = 0$	$h > h_{max}$

TABLE II  
 DIRECTIONS IN WHICH BRIGHTNESS  
 DATA ARE STORED IN THE DATA BASE

k	$\theta_k$ (degrees)	$\phi_k$ (degrees)
1	0	0
2	30	30
3	30	90
4	30	150
5	60	0
6	60	45
7	60	90
8	60	135
9	60	180
10	90	15
11	90	45
12	90	75
13	90	105
14	90	135
15	90	165
16	120	0
17	120	45
18	120	90
19	120	135
20	120	180
21	150	30
22	150	90
23	150	150
24	180	0

The coordinate system is shown in Figure 2.  $\theta$  is the polar angle from the local vertical, and  $\phi$  is the azimuthal angle measured from the plane containing the sun and the local vertical.

TABLE III  
 LOCAL POINTS USED IN THE SPHERICAL CALCULATION

A. SUN ANGLE ( $\lambda_i$ )

0°, 2°, 4°, . . . . . 120°

For  $\lambda \geq 120^\circ$ , all brightness values are set to zero.

B. HEIGHT ( $h_j$ )

j	$h_j$	Optical Thickness Interval
1	0.0	.00
2	122.3035	.0277
3	123.0	.0278
4	123.8	.0278
5	124.6	.0278
6	125.6	.0278
7	126.6	.0278
8	127.7	.0278
9	129.0	.0278
10	130.4	.0278
11	132.1	.0278
12	134.2	.0278
13	136.7	.0278
14	140.2	.0278
15	145.6	.0210
16	153.4	.0097
17	161.2	.0044
18	168.9	.0020
19	176.7	.0009
20	184.5	.0005
21	192.2	.0002
22	200.0	

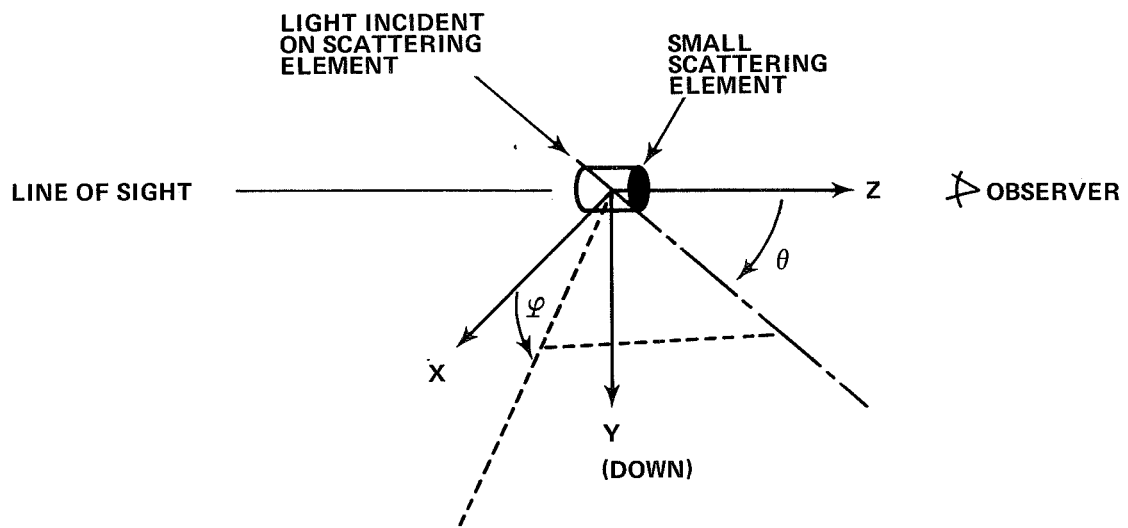


FIGURE 1 - GEOMETRY FOR SCATTERING CALCULATION

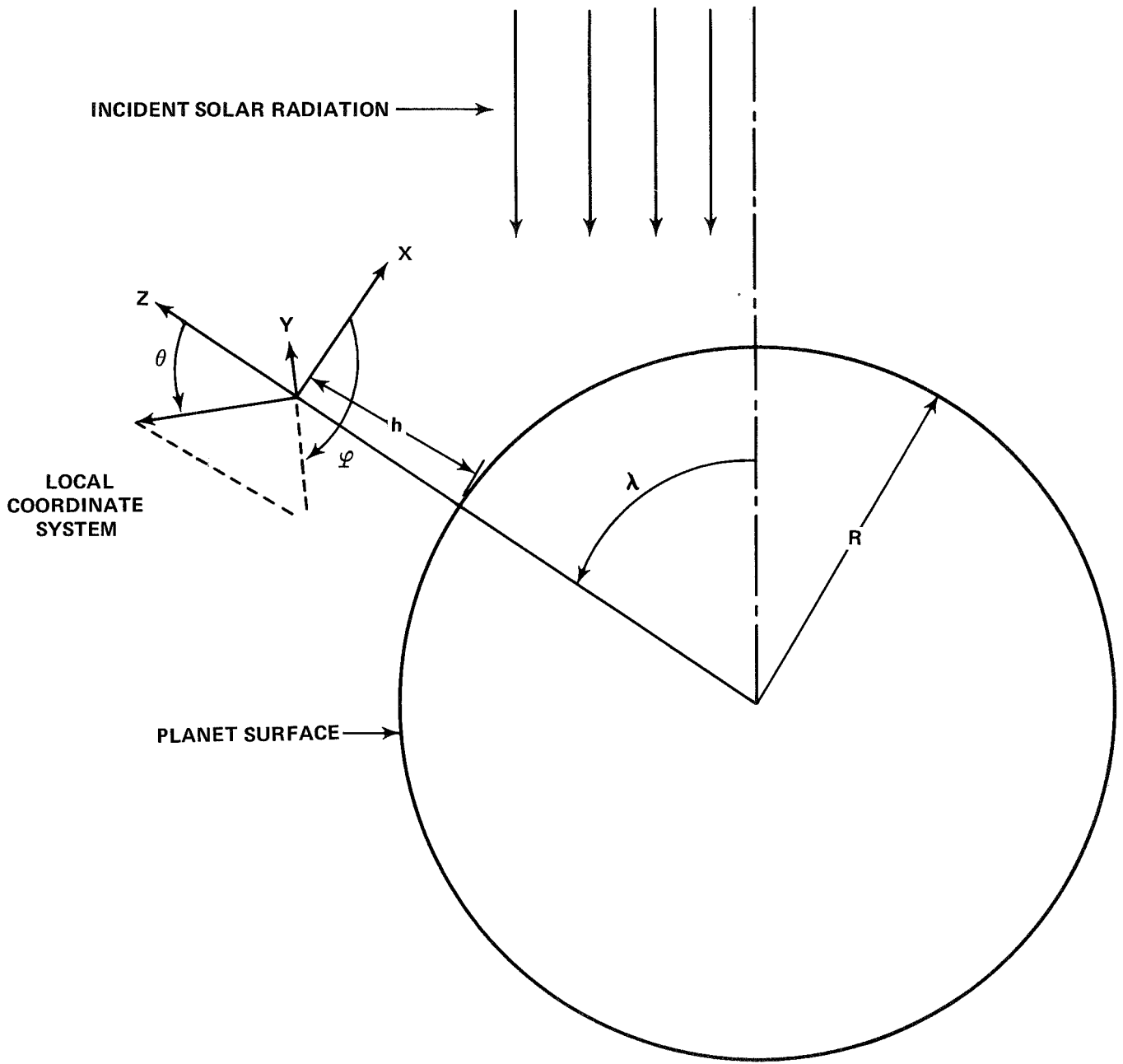


FIGURE 2 - COORDINATE SYSTEM FOR THE DATA BASE

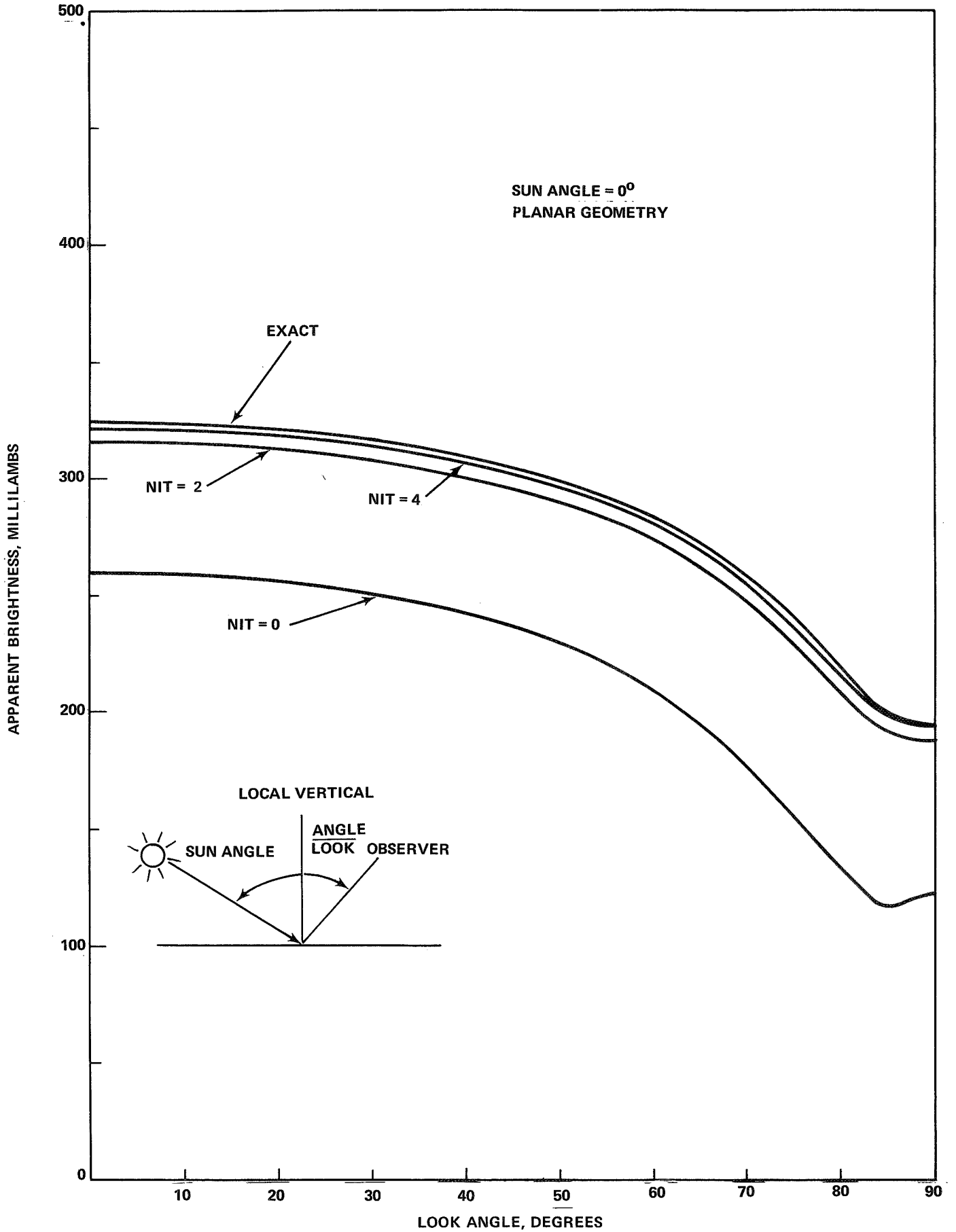


FIGURE 3 - ILLUSTRATION OF THE CONVERGENCE OF THE ITERATIVE CALCULATIONS FOR THE PLANAR HAZE. THE PARAMETER NIT IS THE NUMBER OF ITERATIONS.



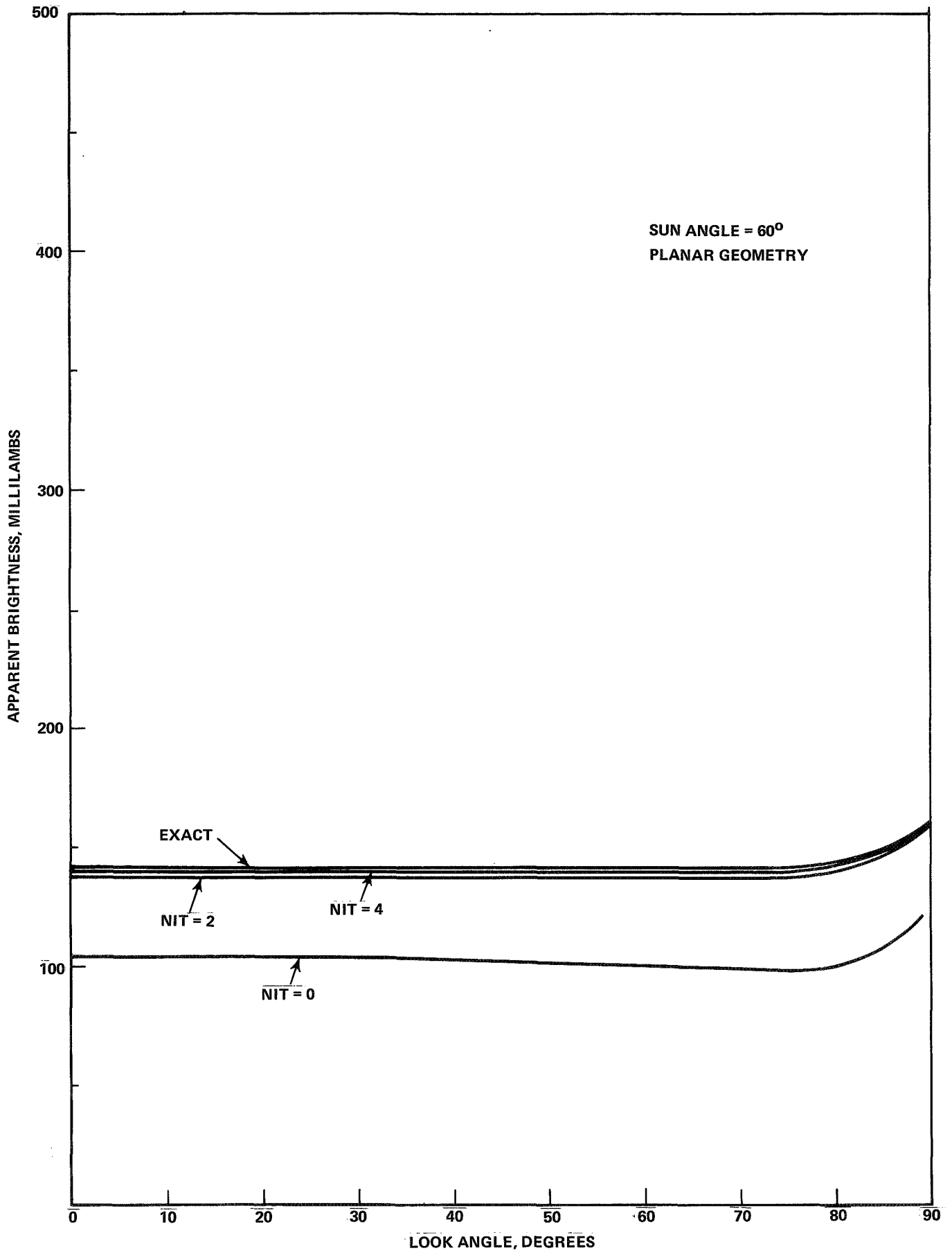


FIGURE 4 - ILLUSTRATION OF THE CONVERGENCE OF THE ITERATIVE CALCULATIONS FOR THE PLANAR HAZE. THE PARAMETER NIT IS THE NUMBER OF ITERATIONS.

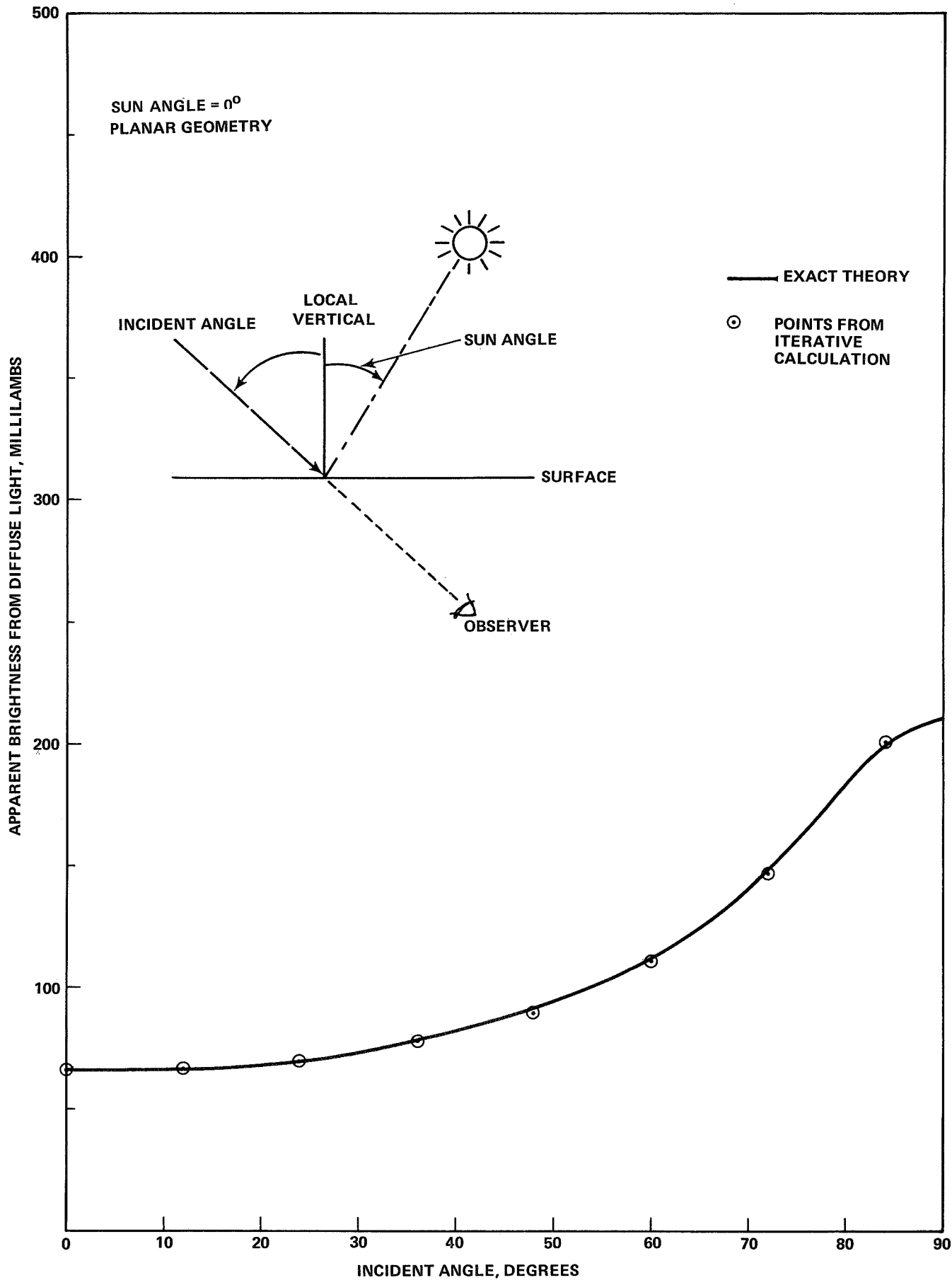


FIGURE 5 - THE INTENSITY OF THE INCIDENT DIFFUSE LIGHT AT THE SURFACE, AS A FUNCTION OF INCIDENCE ANGLE.

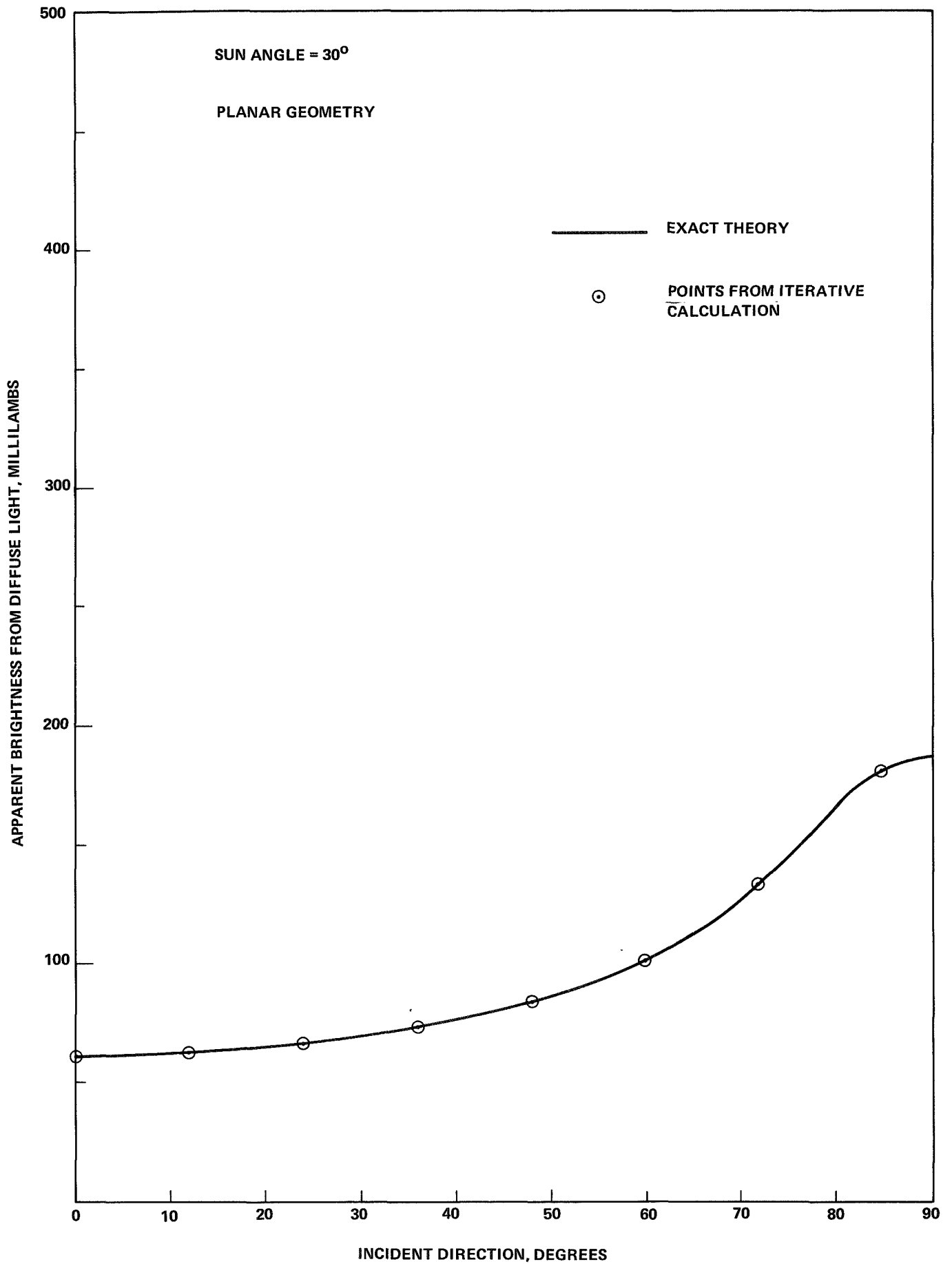
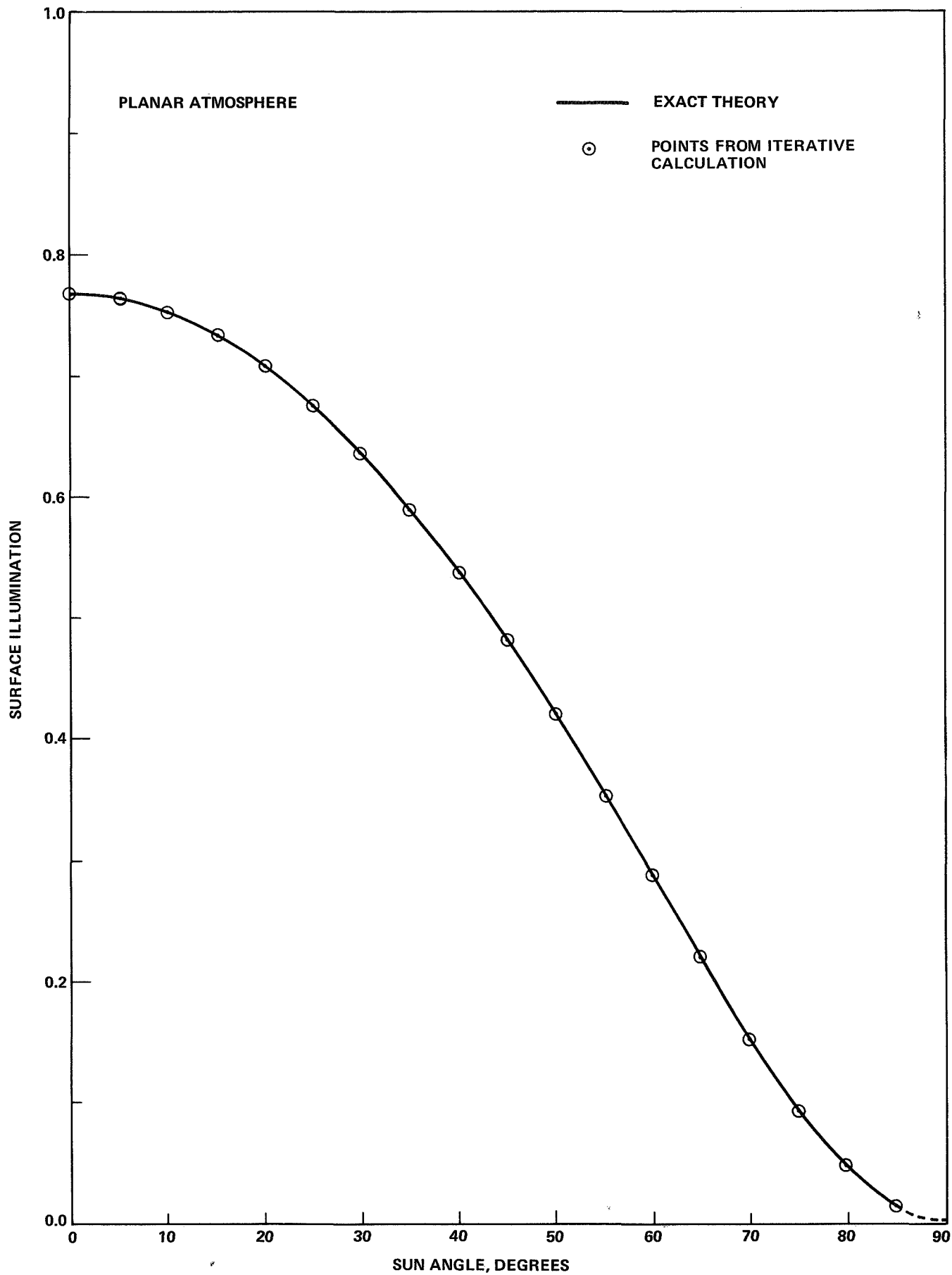


FIGURE 6 - THE INTENSITY OF THE INCIDENT DIFFUSE LIGHT AT THE SURFACE,  
AS A FUNCTION OF THE INCIDENCE ANGLE.



**FIGURE 7 - SURFACE ILLUMINATION AS A FUNCTION OF SUN ANGLE. A VALUE OF UNITY REPRESENTS THE ILLUMINATION OF A SURFACE NORMAL TO THE DIRECT SOLAR RADIATION (WITH NO HAZE).**

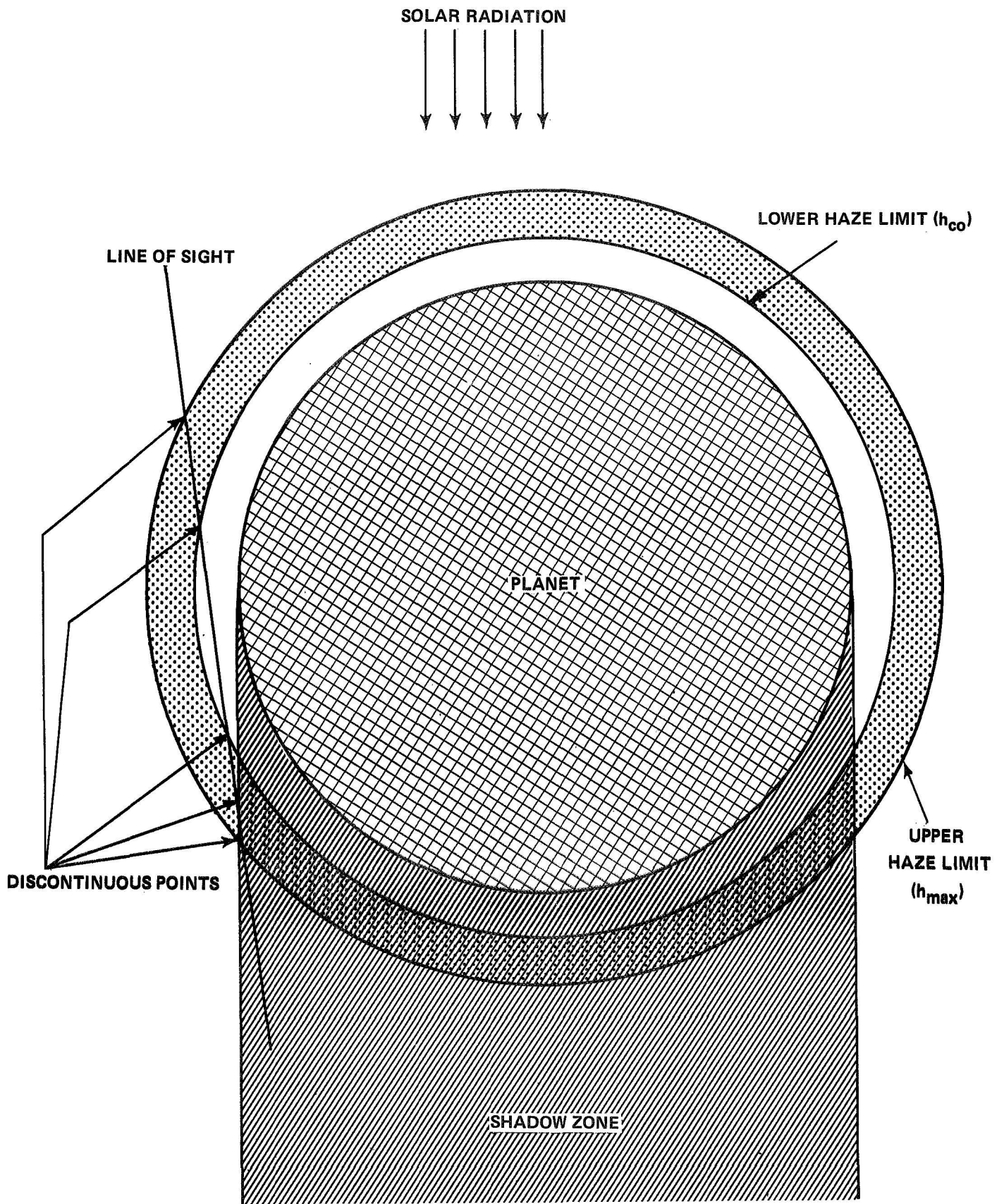


FIGURE 8 - DISCONTINUITIES FOR A TYPICAL LINE OF SIGHT THROUGH THE HAZE

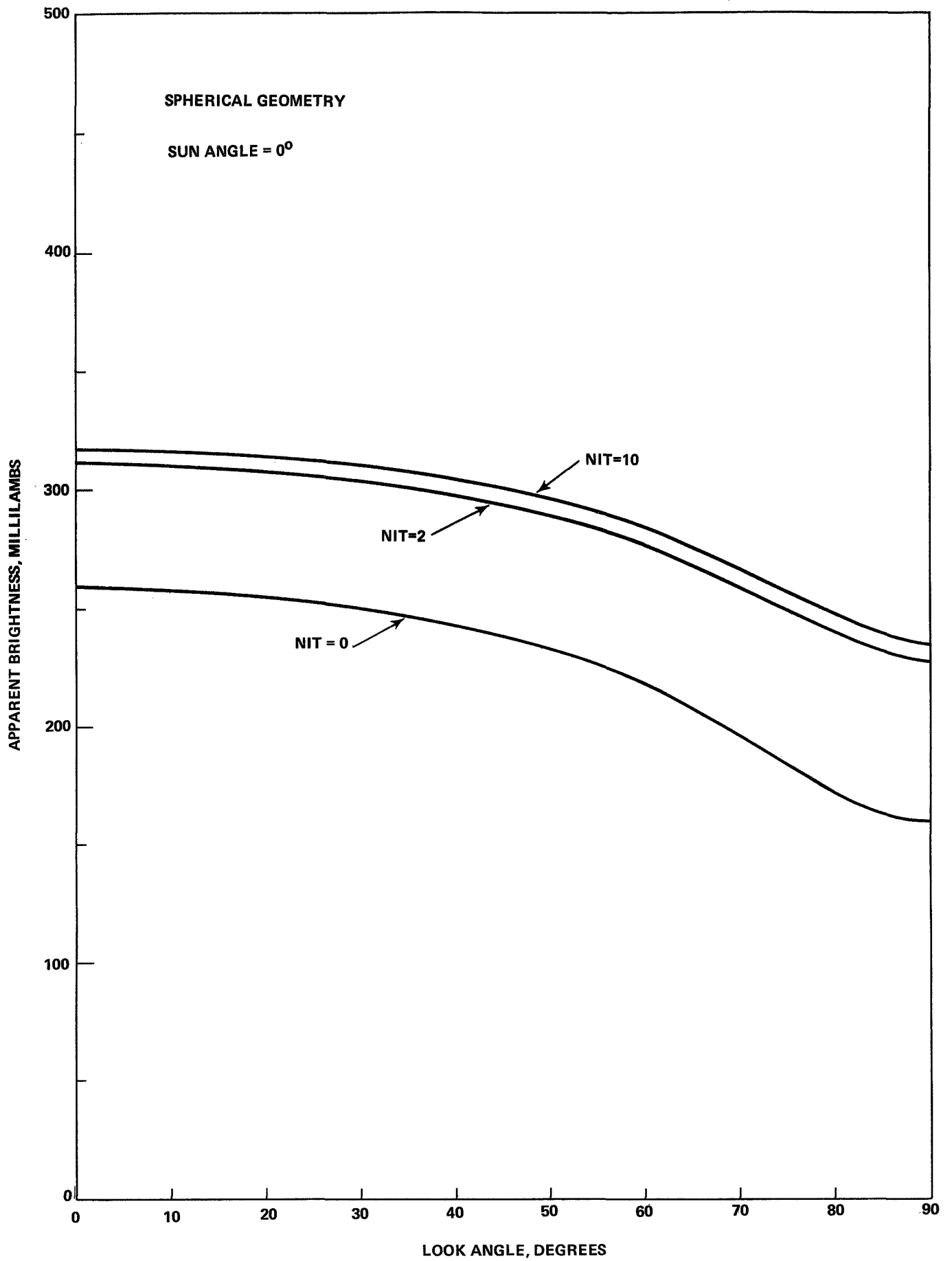


FIGURE 9 - ILLUSTRATION OF THE CONVERGENCE FOR THE SPHERICAL GEOMETRY. NIT INDICATES THE NUMBER OF ITERATIONS.

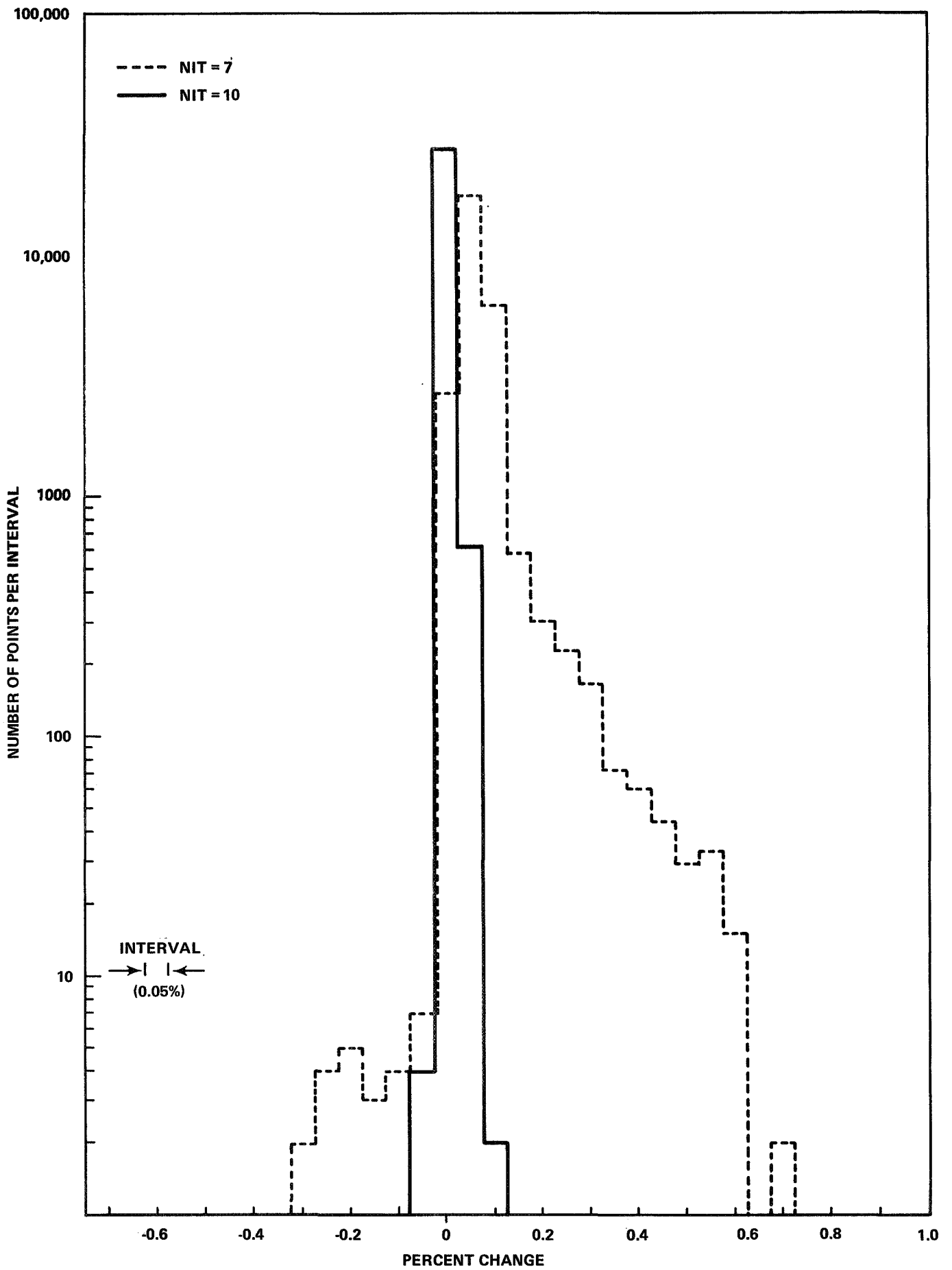


FIGURE 10 - HISTOGRAM SHOWING THE PERCENTAGE CHANGE IN THE POINTS OF THE DATA BASE DUE TO A SINGLE ITERATION. NOTE THE LOGRITHMIC VERTICAL SCALE.

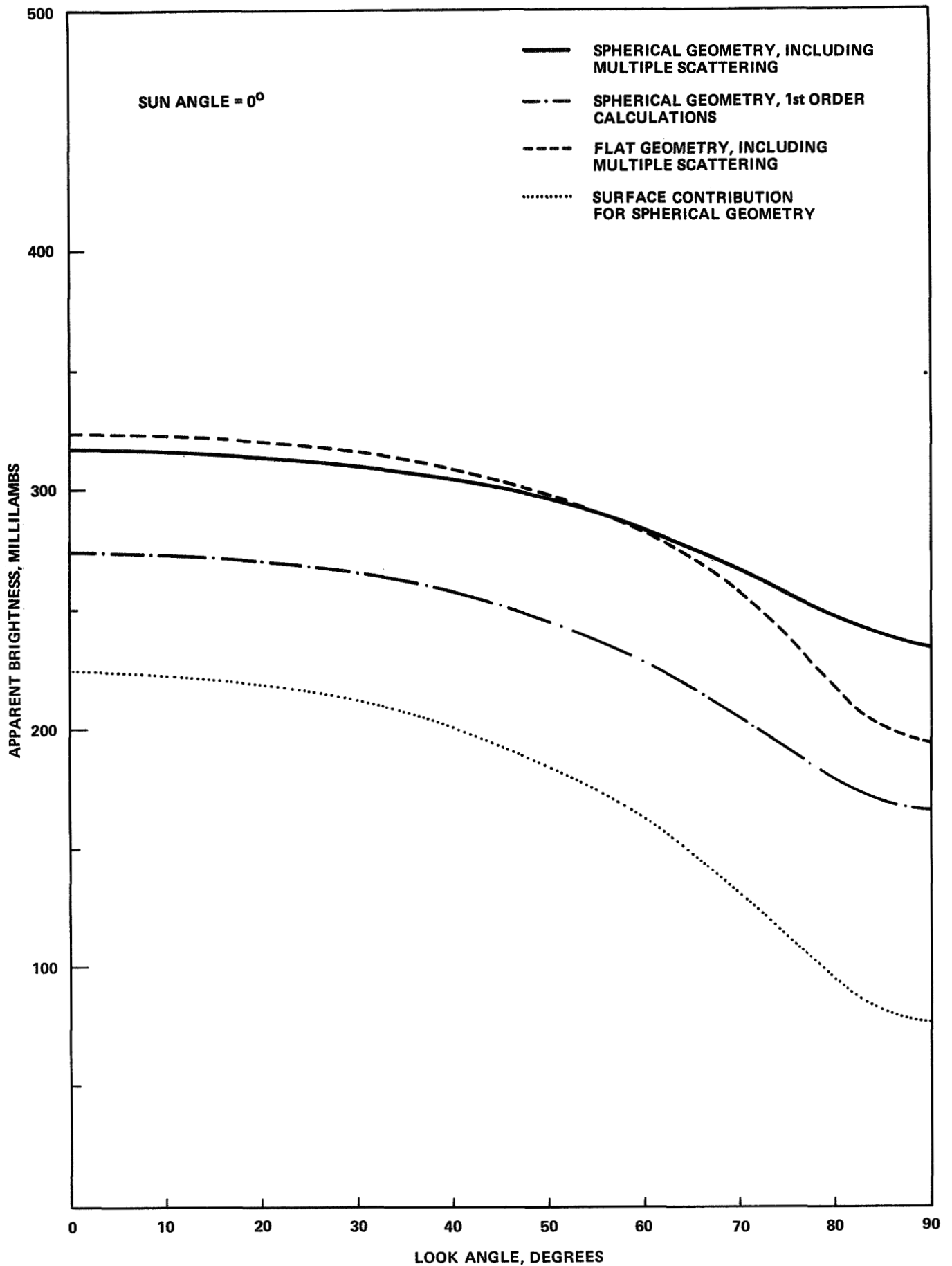


FIGURE 11 - APPARENT BRIGHTNESS, FOR A SUN ANGLE OF 0°, CALCULATED BY SEVERAL DIFFERENT TECHNIQUES.



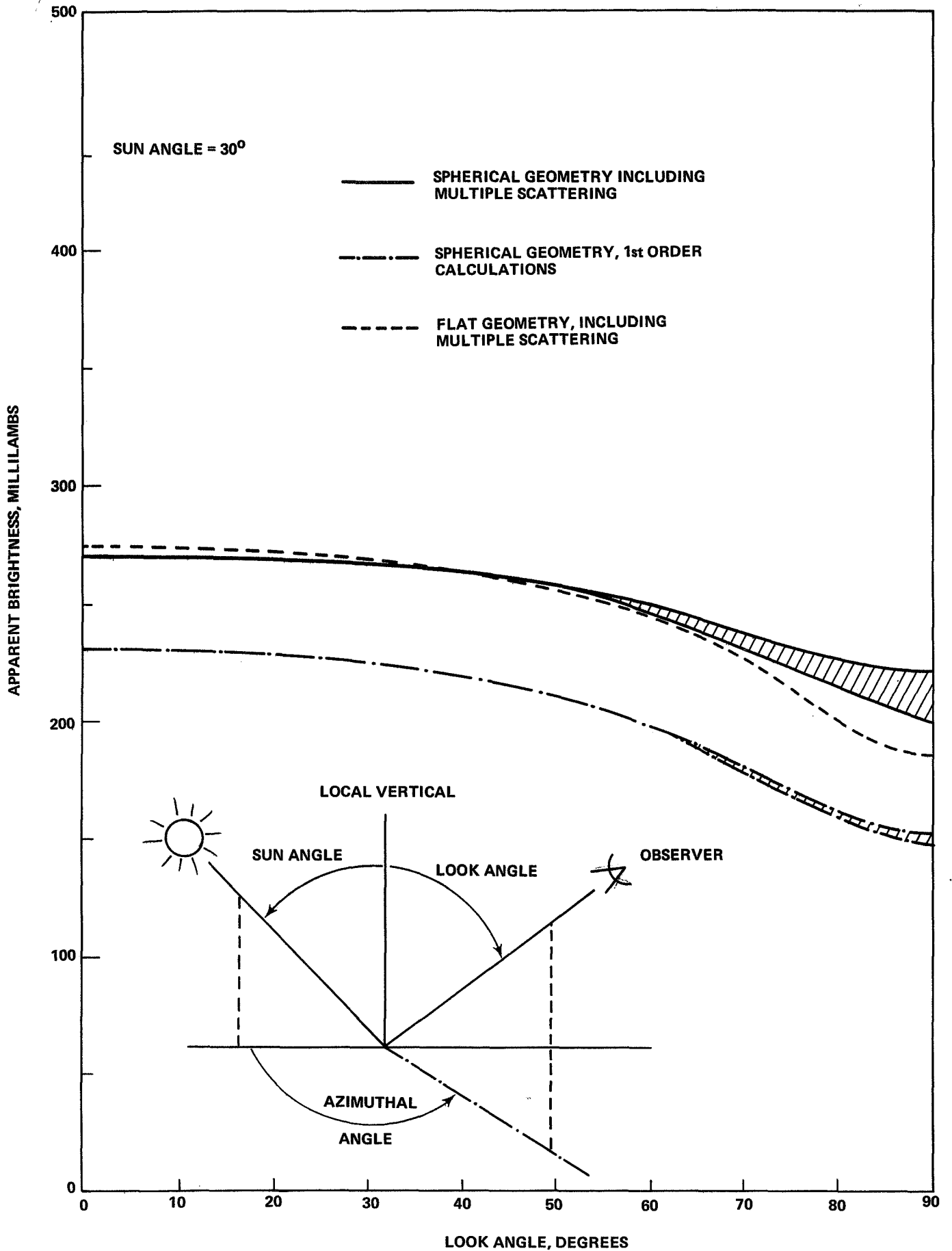


FIGURE 12 - APPARENT BRIGHTNESS FOR A SUN ANGLE OF 30°, CALCULATED BY SEVERAL DIFFERENT TECHNIQUES. THE CROSS-HATCHED AREAS INDICATE THE RANGE OF VARIATION IN THE BRIGHTNESS DUE TO CHANGE IN THE AZIMUTHAL ANGLE.

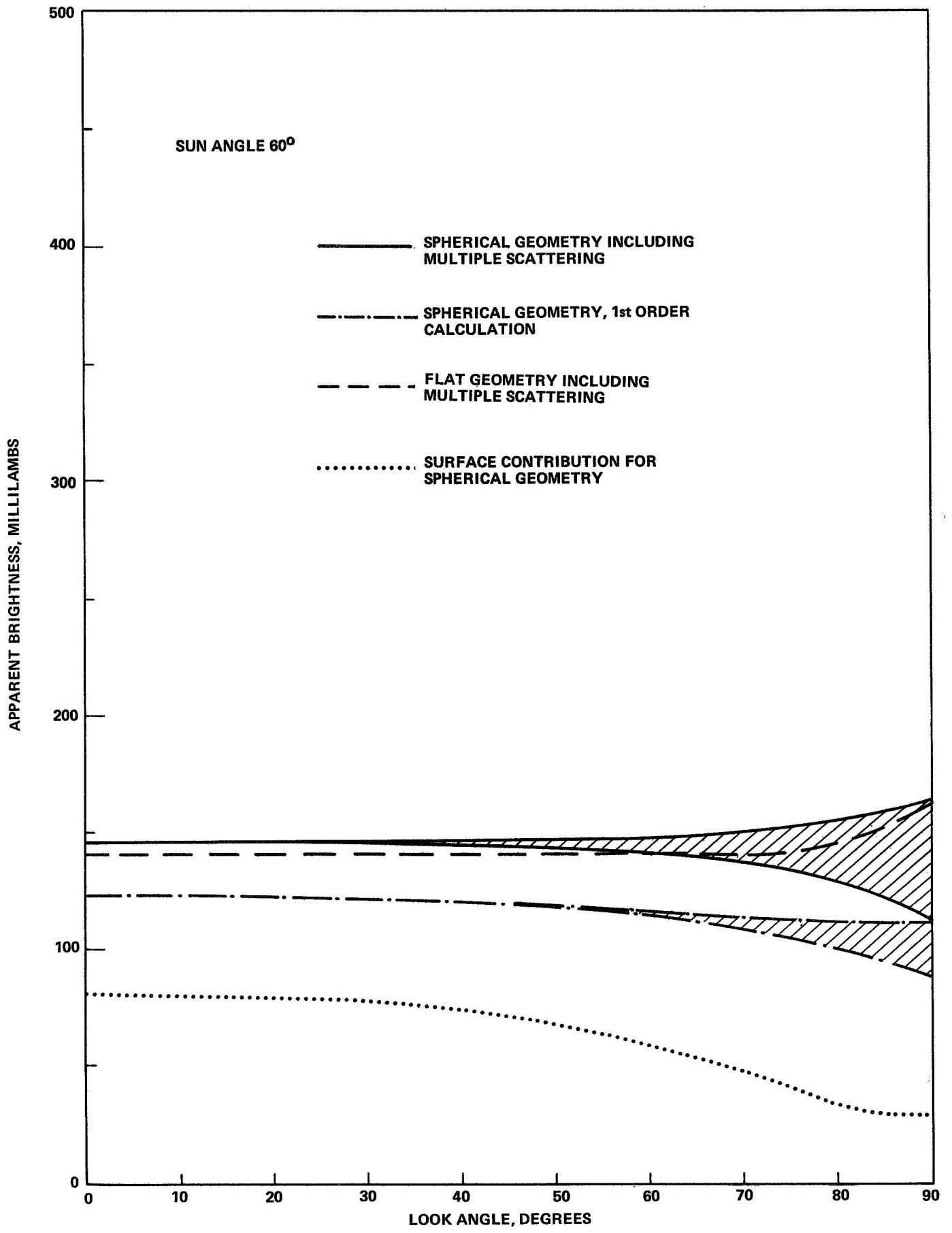
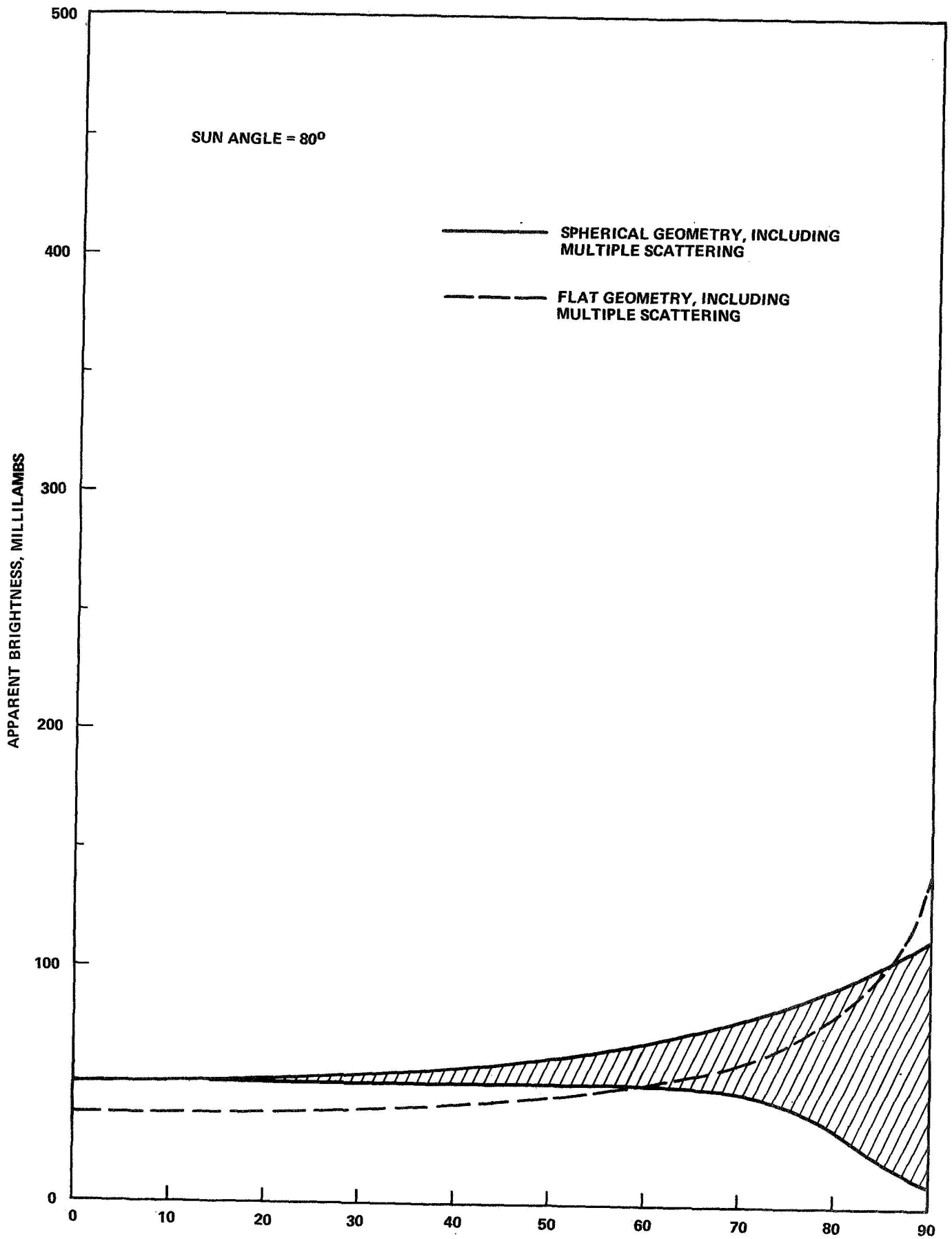


FIGURE 13 - APPARENT BRIGHTNESS FOR A SUN ANGLE OF 60°, CALCULATED BY SEVERAL DIFFERENT TECHNIQUES. THE CROSS-HATCHED AREAS INDICATE THE RANGE OF VARIATION IN THE BRIGHTNESS DUE TO CHANGE IN THE AZIMUTHAL ANGLE.



**FIGURE 14 - APPARENT BRIGHTNESS, FOR A SUN ANGLE OF 80°, CALCULATED BY TWO DIFFERENT TECHNIQUES. THE CROSS-HATCHED AREA INDICATES THE RANGE OF VARIATION IN THE BRIGHTNESS DUE TO CHANGE IN THE AZIMUTHAL ANGLE.**

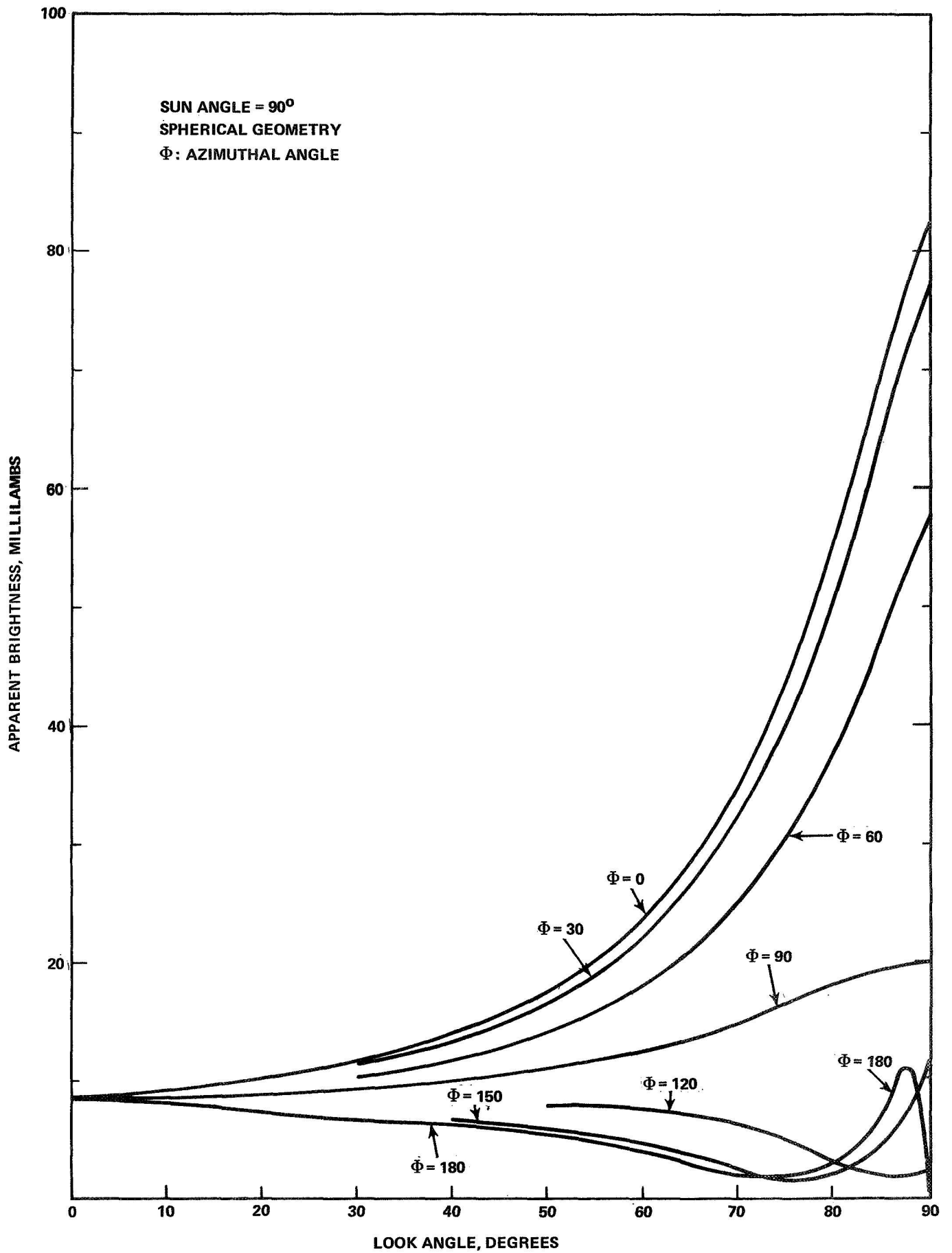


FIGURE 15 - APPARENT BRIGHTNESS FOR SEVERAL VALUES OF THE AZIMUTHAL ANGLE  $\Phi$ . THE VERTICAL SCALE HAS BEEN MAGNIFIED OVER THAT USED IN PREVIOUS FIGURES.

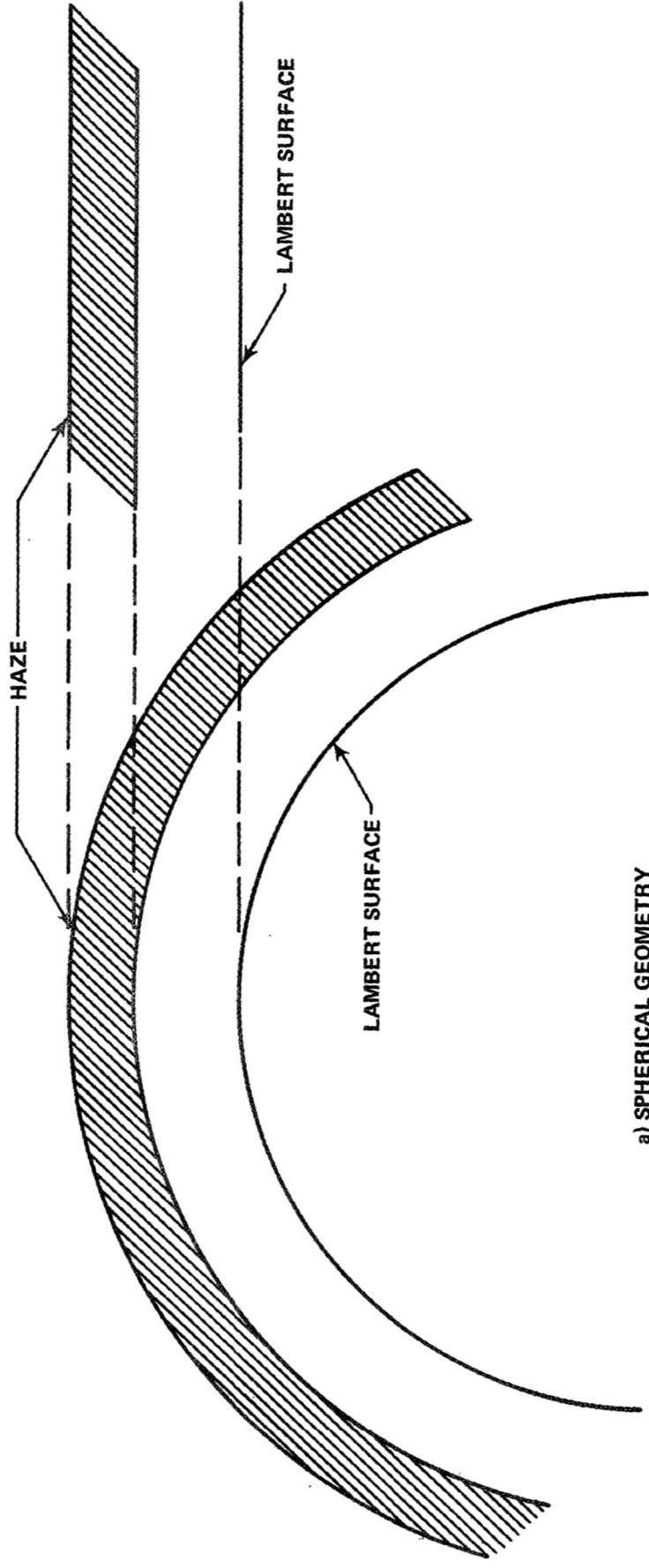
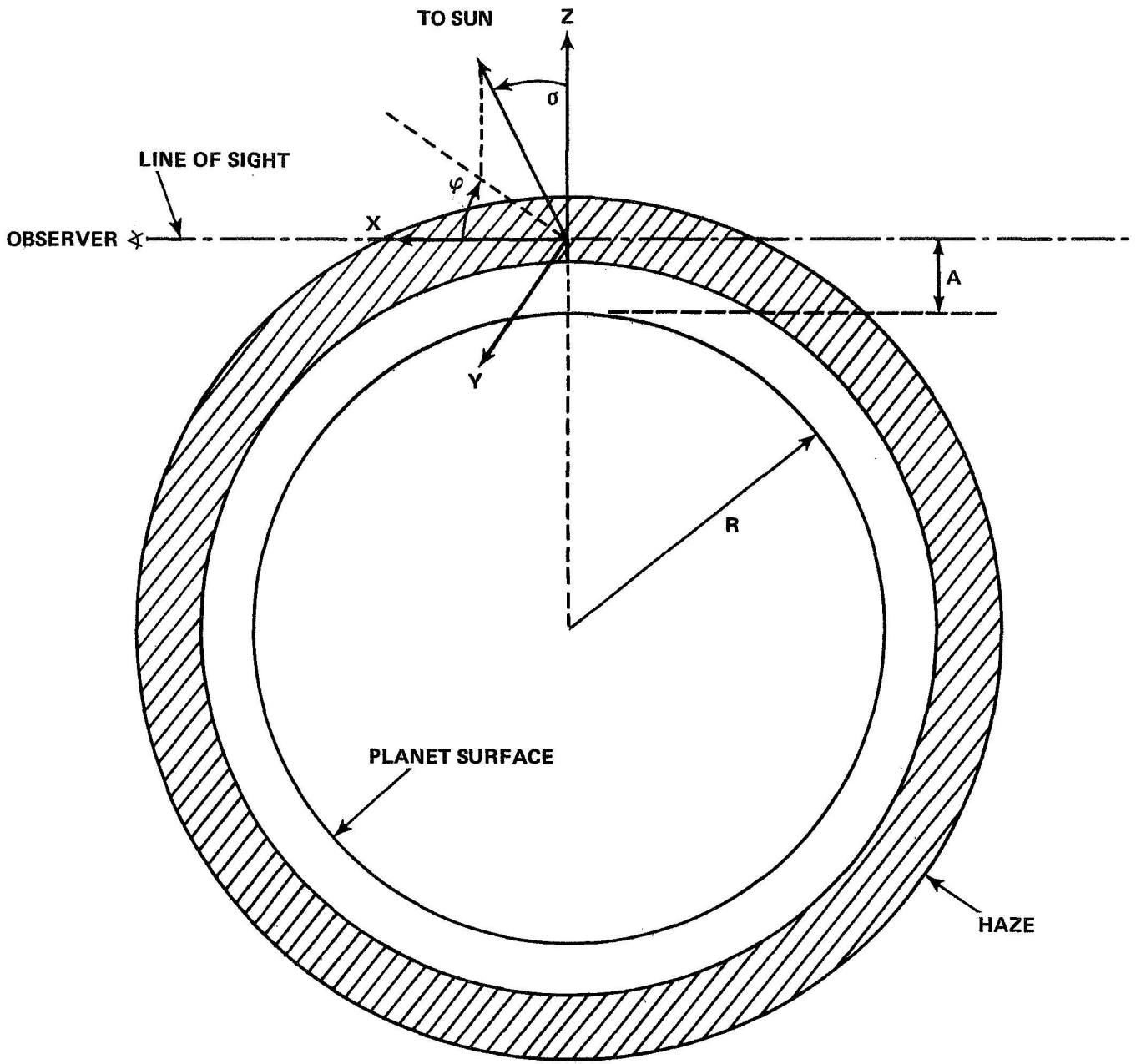
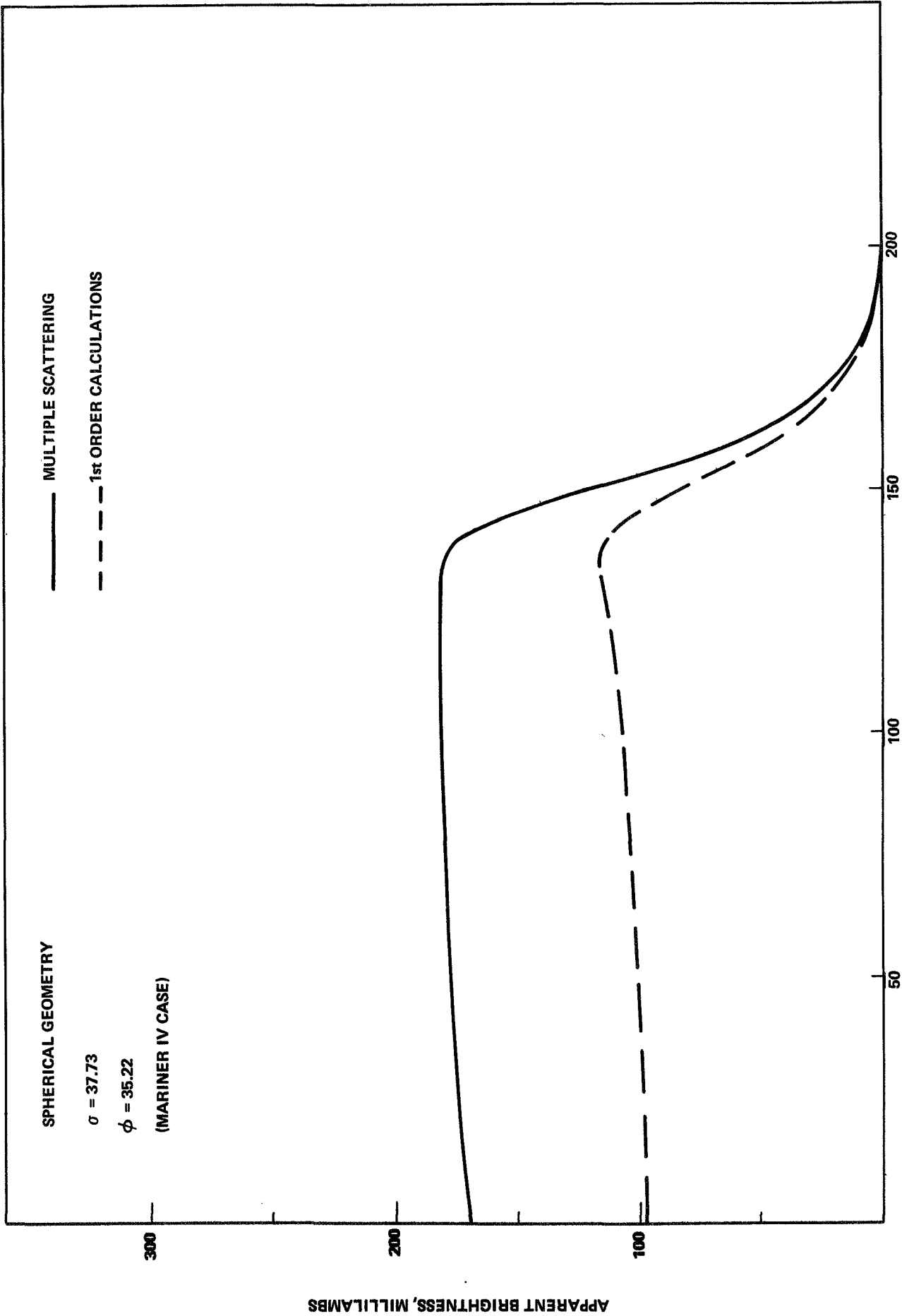


FIGURE 16 - COMPARISON OF THE GEOMETRIES USED FOR THE FLAT AND THE SPHERICAL BRIGHTNESS CALCULATIONS.



**FIGURE 17 - VIEWING GEOMETRY ABOVE THE LIMB OF A PLANET. THE QUANTITY A IS THE HEIGHT OF THE LINE OF SIGHT ABOVE THE LIMB.**



ALTITUDE ABOVE THE LIMB, km.

FIGURE 18 - APPARENT BRIGHTNESS ABOVE THE LIMB OF THE PLANET.

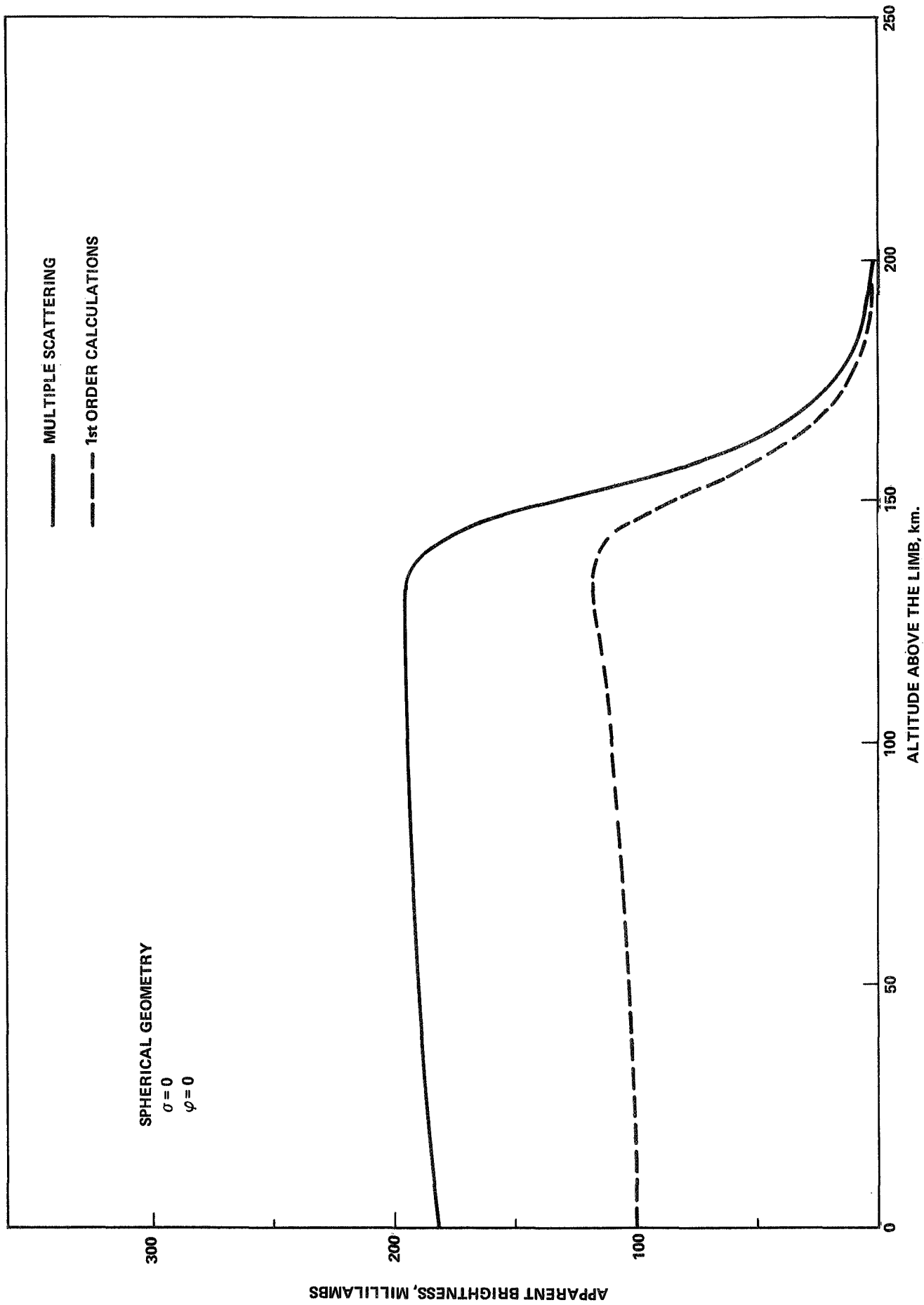


FIGURE 19 - APPARENT BRIGHTNESS ABOVE THE LIMB OF THE PLANET.



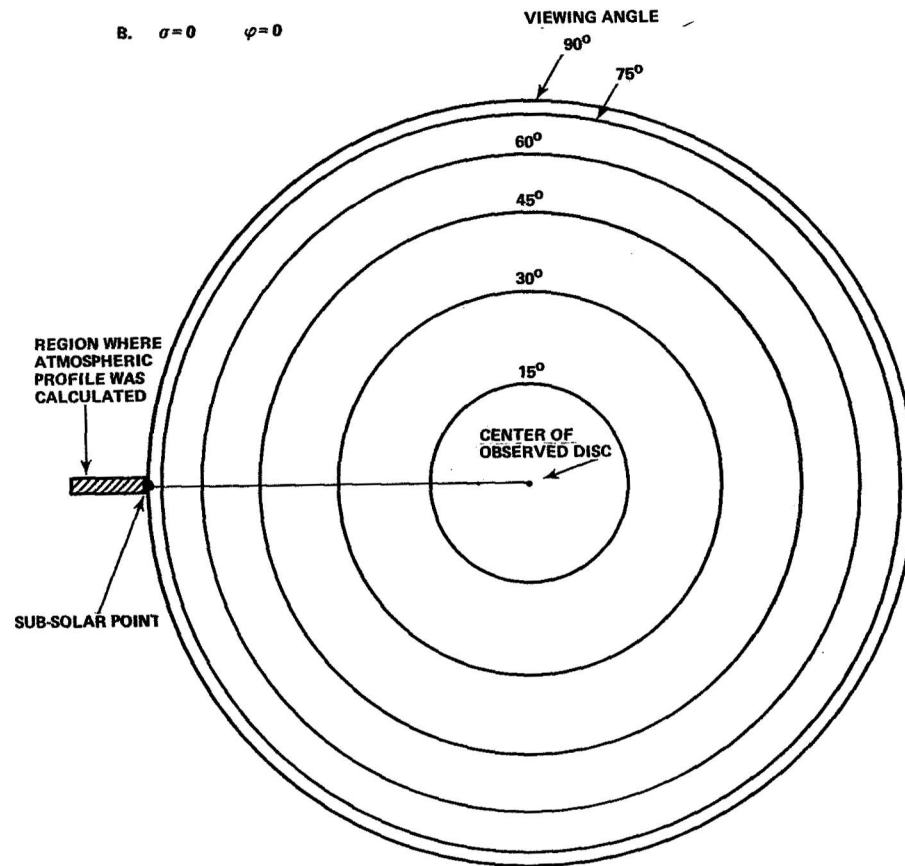
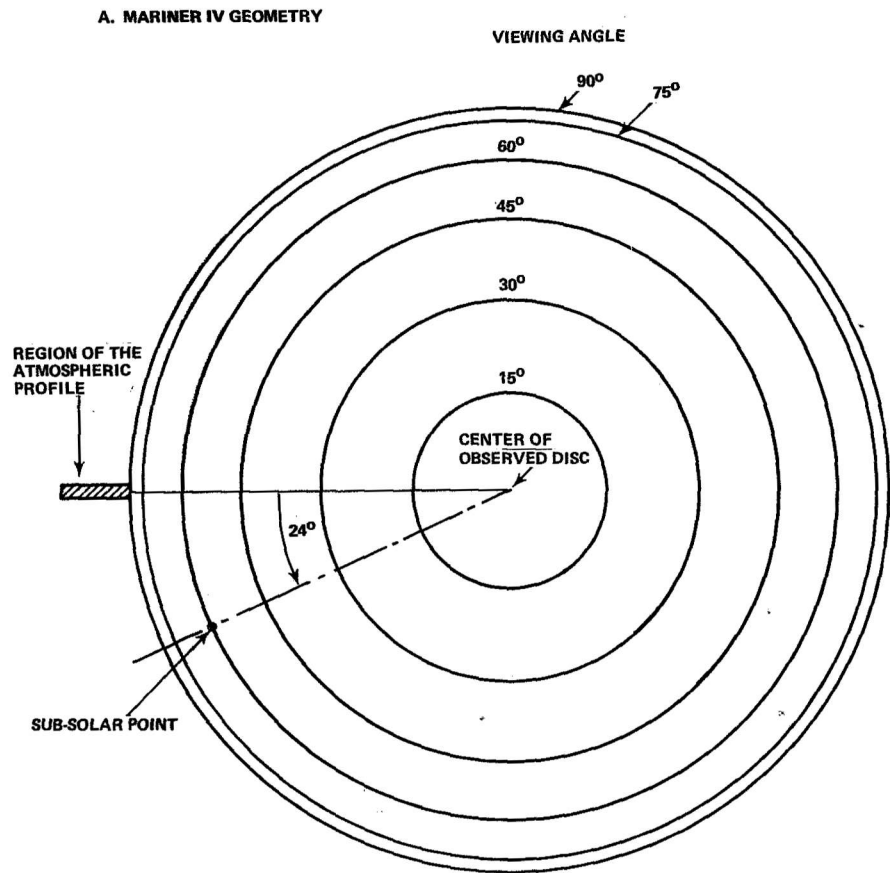


FIGURE 20 - ILLUSTRATION OF THE GEOMETRY USED IN FIGURE 18 (A) AND IN FIGURE 19 (B).

